



University of Groningen

MASTER'S THESIS

Do muscle synergies in the arm change when learning to use a multi-articulate pattern recognition controlled prosthetic hand?

Author:

Alok Ranjan
(s3816494)
Medical Device Design
Biomedical Engineering
University of Groningen

Thesis Supervisor:

dr. R.M. (Raoul) Bongers
Center for Human Movement Sciences
University Medical Center Groningen

University Supervisor:

prof. dr. ir. G.J. (Bart) Verkerke
Rehabilitation-General Department
University Medical Center Groningen

*A thesis submitted in fulfillment of the requirements
for the degree of Master of Science*

in

Biomedical Engineering
with a specialisation in
Medical Device Design

July 10, 2020

Abstract

Learning to use an advanced pattern recognition (PR) based myoelectric prosthesis implies learning to produce high-quality electromyogram (EMG) patterns with distinct, not too variable and highly reliable features [1]. Significant improvements in feature space post-learning is reported in multiple studies, as a result, change in feature space is hypothesized to correlate with the improved performance [2] [3]. Moreover, to make motor learning a modular and efficient experience, it is important that we understand the underlying mechanisms of EMG pattern generation and provide a reasoning for the increase in performance. Muscle synergies that are defined as proportional activation of a group of muscles are proposed to be interneuronal networks involve in controlling the muscles and are organized at the level of spinal cord [4][5]. As per, activation in one muscle in a synergy entails about the activations of other muscles in the group. Hence, muscle synergies can serve as primitives of motor control [6]. Linear combination of muscle synergies and their activation coefficients are capable of describing complex forces and motion patterns in reduced dimensions [7]. We used this information of muscle synergies and activation coefficients to look for the change in them with user learning. We are interested in knowing if their structure changes over learning or not. For that, we established an experiment with a user training exercise in which 20 participants learned to control a virtual prosthesis via. a myoelectric controlled interface over 15-training sessions. EMG data from 8-muscles in the hand were recorded. We assessed the recorded muscle data with non-negative matrix factorization (NMF) to extract underlying muscle synergies and muscle activation coefficient patterns. Muscle synergies were matched to its precursor synergies with normalized dot product (NDP) and cosine of principal angles (CPA), and the change in their structure was tracked. Though, recurring solutions were not achieving for all participants, a successful and logical tracking could get achieved for a few participants with k-means clustering of muscle synergies. A mathematical measure of change from initial averaged behavior to final averaged behavior for muscle synergies was also calculated with CPA. Activation coefficients were also tracked, based on the matching of muscle synergies. The change in muscle activation coefficient patterns was expressed in terms of mean \pm SD. This represented that muscle synergies and muscle activation coefficient patterns both change with user learning.

Contents

Abstract	i
List of Figures	ix
List of Tables	x
Acknowledgements	xi
Declaration	xiii
1 Introduction	1
2 Materials and Methods	6
2.1 Participants	6
2.2 Myoelectric machine learning system	6
2.3 Procedure	7
2.4 The dataset	7
2.5 Data Analysis	7
2.5.1 Pre-processing	7
2.5.2 Muscle synergies' model and NMF	8
2.5.3 Muscle synergy extraction criteria	9
2.5.3.1 Dimensionality analysis	9
2.5.4 Simulated data: Is 8-channel data enough to apply NMF? . .	10
2.5.5 Simple vs Forced solutions via NMF	11
2.5.6 Similarity analysis	11

3 Results	13
3.1 Dimensionality analysis	13
3.2 Simulated data vs Observed data	14
3.2.1 Simple vs Forced solutions via NMF	16
3.3 Similarity analysis	17
3.3.1 <i>NDP and CPA</i>	17
3.3.2 <i>k-means Clustering</i>	18
4 Discussion	26
5 Conclusion	30
Ethics	31
Appendix-1	32
Bibliography	52

List of Figures

3.1	Graphical representation of muscle synergy extraction: variance explained for (VAF) versus number of synergies (k)	13
3.2	Histograms of (1) an 8-channel observed data, (2) an 8-channel simulated data, and (3) a 22-channel simulated data	14
3.3	Bar-graphs of four muscle synergies (W1-W4) over training sessions (tr) for participant 9, matching is done by NDP (or CPA), m_1 to m_8 on x-axis represent 8-muscles, bars show the fixed muscle synergy activations of muscles	18
3.4	Change in four activation coefficient patterns (H1-H4) over training sessions (tr) for participant 9, matching is adopted from the matching of related muscle synergies, X-axis represents number of total observed points	19
3.5	Graphical representation of muscle synergy structure: four different colors show four muscle synergy structures and the activation scales are mentioned on the axes.	20
3.6	Spider plot for P3: different colors show the different synergies (W1-W4). Top (training session 1-5), mid (training session 6-10) and bottom (training session 11-15). A change in the muscle synergy activation and distribution can be noticed from training session 1 to training session 15. Matching is done by k-means clustering.	21
3.7	Spider plot for P19: different colors show the different synergies (W1-W4). Top (training session 1-5), mid (training session 6-10) and bottom (training session 11-15). A change in the muscle synergy activation and distribution can be noticed from training session 1 to training session 15. Matching is done by k-means clustering.	22
3.8	Change in four activation coefficient patterns (H1-H4) over training sessions (tr) for participant 3, matching is done by k-means clustering of muscle synergies	22

3.9	Change in four activation coefficient patterns (H1-H4) over training sessions (tr) for participant 19, matching is done by k-means clustering of muscle synergies	23
5.1	Bar-graphs of four muscle synergies (W1-W4) over training sessions (tr) for participant 1, matching is done by NDP (or CPA), m_1 to m_8 on x-axis represent 8-muscles, bars show the fixed muscle synergy activations of muscles	32
5.2	Bar-graphs of four muscle synergies (W1-W4) over training sessions (tr) for participant 2, matching is done by NDP (or CPA), m_1 to m_8 on x-axis represent 8-muscles, bars show the fixed muscle synergy activations of muscles	33
5.3	Bar-graphs of four muscle synergies (W1-W4) over training sessions (tr) for participant 3, matching is done by NDP (or CPA), m_1 to m_8 on x-axis represent 8-muscles, bars show the fixed muscle synergy activations of muscles	33
5.4	Bar-graphs of four muscle synergies (W1-W4) over training sessions (tr) for participant 4, matching is done by NDP (or CPA), m_1 to m_8 on x-axis represent 8-muscles, bars show the fixed muscle synergy activations of muscles	34
5.5	Bar-graphs of four muscle synergies (W1-W4) over training sessions (tr) for participant 5, matching is done by NDP (or CPA), m_1 to m_8 on x-axis represent 8-muscles, bars show the fixed muscle synergy activations of muscles	34
5.6	Bar-graphs of four muscle synergies (W1-W4) over training sessions (tr) for participant 6, matching is done by NDP (or CPA), m_1 to m_8 on x-axis represent 8-muscles, bars show the fixed muscle synergy activations of muscles	35
5.7	Bar-graphs of four muscle synergies (W1-W4) over training sessions (tr) for participant 7, matching is done by NDP (or CPA), m_1 to m_8 on x-axis represent 8-muscles, bars show the fixed muscle synergy activations of muscles	35
5.8	Bar-graphs of four muscle synergies (W1-W4) over training sessions (tr) for participant 8, matching is done by NDP (or CPA), m_1 to m_8 on x-axis represent 8-muscles, bars show the fixed muscle synergy activations of muscles	36

5.9 Bar-graphs of four muscle synergies (W1-W4) over training sessions (tr) for participant 10, matching is done by NDP (or CPA), m_1 to m_8 on x-axis represent 8-muscles, bars show the fixed muscle synergy activations of muscles	36
5.10 Bar-graphs of four muscle synergies (W1-W4) over training sessions (tr) for participant 11, matching is done by NDP (or CPA), m_1 to m_8 on x-axis represent 8-muscles, bars show the fixed muscle synergy activations of muscles	37
5.11 Bar-graphs of four muscle synergies (W1-W4) over training sessions (tr) for participant 12, matching is done by NDP (or CPA), m_1 to m_8 on x-axis represent 8-muscles, bars show the fixed muscle synergy activations of muscles	37
5.12 Bar-graphs of four muscle synergies (W1-W4) over training sessions (tr) for participant 13, matching is done by NDP (or CPA), m_1 to m_8 on x-axis represent 8-muscles, bars show the fixed muscle synergy activations of muscles	38
5.13 Bar-graphs of four muscle synergies (W1-W4) over training sessions (tr) for participant 14, matching is done by NDP (or CPA), m_1 to m_8 on x-axis represent 8-muscles, bars show the fixed muscle synergy activations of muscles	38
5.14 Bar-graphs of four muscle synergies (W1-W4) over training sessions (tr) for participant 15, matching is done by NDP (or CPA), m_1 to m_8 on x-axis represent 8-muscles, bars show the fixed muscle synergy activations of muscles	39
5.15 Bar-graphs of four muscle synergies (W1-W4) over training sessions (tr) for participant 16, matching is done by NDP (or CPA), m_1 to m_8 on x-axis represent 8-muscles, bars show the fixed muscle synergy activations of muscles	39
5.16 Bar-graphs of four muscle synergies (W1-W4) over training sessions (tr) for participant 17, matching is done by NDP (or CPA), m_1 to m_8 on x-axis represent 8-muscles, bars show the fixed muscle synergy activations of muscles	40
5.17 Bar-graphs of four muscle synergies (W1-W4) over training sessions (tr) for participant 18, matching is done by NDP (or CPA), m_1 to m_8 on x-axis represent 8-muscles, bars show the fixed muscle synergy activations of muscles	40

5.18 Bar-graphs of four muscle synergies (W1-W4) over training sessions (tr) for participant 19, matching is done by NDP (or CPA), m_1 to m_8 on x-axis represent 8-muscles, bars show the fixed muscle synergy activations of muscles	41
5.19 Bar-graphs of four muscle synergies (W1-W4) over training sessions (tr) for participant 20, matching is done by NDP (or CPA), m_1 to m_8 on x-axis represent 8-muscles, bars show the fixed muscle synergy activations of muscles	41
5.20 Change in four activation coefficient patterns (H1-H4) over training sessions (tr) for participant 1, matching is adopted from the matching of related muscle synergies, X-axis represents number of total observed points	42
5.21 Change in four activation coefficient patterns (H1-H4) over training sessions (tr) for participant 2, matching is adopted from the matching of related muscle synergies, X-axis represents number of total observed points	42
5.22 Change in four activation coefficient patterns (H1-H4) over training sessions (tr) for participant 3, matching is adopted from the matching of related muscle synergies, X-axis represents number of total observed points	43
5.23 Change in four activation coefficient patterns (H1-H4) over training sessions (tr) for participant 4, matching is adopted from the matching of related muscle synergies, X-axis represents number of total observed points	43
5.24 Change in four activation coefficient patterns (H1-H4) over training sessions (tr) for participant 5, matching is adopted from the matching of related muscle synergies, X-axis represents number of total observed points	44
5.25 Change in four activation coefficient patterns (H1-H4) over training sessions (tr) for participant 6, matching is adopted from the matching of related muscle synergies, X-axis represents number of total observed points	44
5.26 Change in four activation coefficient patterns (H1-H4) over training sessions (tr) for participant 7, matching is adopted from the matching of related muscle synergies, X-axis represents number of total observed points	45

5.27 Change in four activation coefficient patterns (H1-H4) over training sessions (tr) for participant 8, matching is adopted from the matching of related muscle synergies, X-axis represents number of total observed points	45
5.28 Change in four activation coefficient patterns (H1-H4) over training sessions (tr) for participant 10, matching is adopted from the matching of related muscle synergies, X-axis represents number of total observed points	46
5.29 Change in four activation coefficient patterns (H1-H4) over training sessions (tr) for participant 11, matching is adopted from the matching of related muscle synergies, X-axis represents number of total observed points	46
5.30 Change in four activation coefficient patterns (H1-H4) over training sessions (tr) for participant 12, matching is adopted from the matching of related muscle synergies, X-axis represents number of total observed points	47
5.31 Change in four activation coefficient patterns (H1-H4) over training sessions (tr) for participant 13, matching is adopted from the matching of related muscle synergies, X-axis represents number of total observed points	47
5.32 Change in four activation coefficient patterns (H1-H4) over training sessions (tr) for participant 14, matching is adopted from the matching of related muscle synergies, X-axis represents number of total observed points	48
5.33 Change in four activation coefficient patterns (H1-H4) over training sessions (tr) for participant 15, matching is adopted from the matching of related muscle synergies, X-axis represents number of total observed points	48
5.34 Change in four activation coefficient patterns (H1-H4) over training sessions (tr) for participant 16, matching is adopted from the matching of related muscle synergies, X-axis represents number of total observed points	49
5.35 Change in four activation coefficient patterns (H1-H4) over training sessions (tr) for participant 17, matching is adopted from the matching of related muscle synergies, X-axis represents number of total observed points	49

5.36 Change in four activation coefficient patterns (H1-H4) over training sessions (tr) for participant 18, matching is adopted from the matching of related muscle synergies, X-axis represents number of total observed points	50
5.37 Change in four activation coefficient patterns (H1-H4) over training sessions (tr) for participant 19, matching is adopted from the matching of related muscle synergies, X-axis represents number of total observed points	50
5.38 Change in four activation coefficient patterns (H1-H4) over training sessions (tr) for participant 20, matching is adopted from the matching of related muscle synergies, X-axis represents number of total observed points	51

List of Tables

3.1	Number of synergies vs VAF and its cumulative difference	14
3.2	Cluster size for each participant by k-means	20
3.3	From initial to final averaged solution, angular change (CPA) in synergy structure for each participant	24
3.4	Initial and final averaged solutions of activation coefficient patterns, represented in form of mean±SD for each participant	25

Acknowledgements

I would like to acknowledge my sincere gratitude to my supervisor, Dr. Raoul Bongers, for providing me an opportunity to work with him on a topic that I have had minimal experience. I also am thankful for his guidance and explanations that made me learn new things in the field of Neural Engineering.

I am very much thankful to Prof. Dr. Natasha Maurits and Ms. Joyce Weersink for their initial assistance in understanding biological signal processing during my internship.

I also would like to thank Tim A. Valk for his sincere replies to my e-mails and helping me out to understand his published work.

I will never express enough gratitude to my family and my close friends for their unconditional love, endless support, and inspiration. But, I would like to extend my sincere thanks to Shubham, Devlina, Kanishk, Parth and Zeus for sticking around and helping me emotionally or in academia.

पढ़ पढ़ आलिम फ़ाज़िल होइओं,
 कदे अपने आप नूं पढ़आई नही।
 जा जा वडाए मन्दिर मसीती,
 कदे मन अपने विच बड़याई नही।
 ऐवें रोज़ शैतान नाल लड़नै,
 कदे नफ़स अपने नाल लड़याई नही।
 बुल्हे शाह असमानी उडदियां फ़ड़नै,
 जेहड़ा घर बैठा उहनूं फ़ड़याई नही।

- बुल्हे शाह

You read to become a scholar,
 But you never read yourself.

You run to enter your mosques and temples,
 But you never entered your own heart.

Everyday you fight Satan for what,
 You have never fought your own Ego.

Bulleh Shah you try grabbing that which is in the sky,
 But you never get hold of what sits inside yourself.

-Bulleh Shah

Declaration

I, Alok Ranjan, declare that this thesis titled, "Do muscle synergies in the arm change when learning to use a multi-articulate pattern recognition controlled prosthetic hand?" is a presentation of original work and I am the sole author. This work has not previously been presented for an award at this, or any other, University. All sources are acknowledged as references.

Signed:



Date:

July 10, 2020

Place:

Groningen

Chapter 1

Introduction

Learning to control an advanced myoelectric prosthetic hand is similar to learning a new motor skill. Brain plasticity allows for the change into the neuromuscular system, and as a result, with learning, users change control commands permanently[8]. These control commands result in the activation of muscle sites, where electrodes of a prosthesis sit on the remnant muscles of the amputated limb to record the surface electromyographic (sEMG) signals. Myoelectric-upper-limb-prostheses have advanced from simple, direct-controlled, one degree of freedom (DOF) mechanisms (such as grippers) to multiarticulate prosthetic hands controlled with pattern recognition (PR) techniques [7]. PR techniques decode a mapping between EMG signals and multiple hand movements to provide intuitive control of multiple DOFs [9]. For successful functionality, PR techniques require the user to generate high-quality EMG patterns (i.e., EMG patterns with consistent and separable features). An inability in replicating EMG patterns leads to a decrement in the control performance [1]. To accommodate for the variability in EMG pattern generation, various control algorithms have been implemented for correct movement prediction. But even after that, the control is not in a very advanced stage. This is because the previously theorized intuitive control is non-intuitive [6], and the development is more algorithm centric rather than being user-centric. Controlling a prosthesis is complex and therefore, only changing control algorithms is not a route to increase the functionality. We have to bring the user into the scenario so that the user can learn to produce high-quality EMG patterns. This combined effort of learning to produce high-quality EMG patterns and advancing algorithms will make the prosthetic control more robust. Training exercises can help the user learn to produce high-quality EMG patterns, and as a result, changing activation patterns of the muscle sites used to control a prosthesis [10] [11]. Though there is evidence that training changes muscle activation patterns, little is known about learning what leads to which changes in control commands.

Therefore, if we want to optimize learning, we need to know how the activations of these control commands change over learning and what underlying factors cause the permanent change in these control commands that improves the performance. The activation of multiple muscles in hand is organized in the form of muscle synergies and is defined as proportional activation of a group of muscles [4][12]. It can be hypothesized that the proportional activation of muscles (i.e. muscle synergies) changes permanently over learning. Therefore, the goal of this study is to use this information of proportional activation of muscles with training exercises to look for the changes in control commands over learning and try to answer what causes the change in these control commands.

Myoelectric control as a potential control mechanism for assistive devices gained first attention in the 1960s [13][14]. A human-machine interaction was established using SEMG signals that represent nearby motor unit action potentials. These signals are peripheral measurements that contain the neural and peripheral information sent from the spinal cord to the muscles. In principle, this information can be used to determine users' intent and provide control of assistive devices such as active prostheses. For that, two control approaches are currently being used in myoelectric prosthesis: Direct control and Pattern Recognition [15].

Direct controlled prostheses acquire EMG signals from a group of residual antagonistic flexor and extensor muscles. This allows for an actuator to open and close, providing movement in one degree of freedom (DOF), which with conjunction of switching techniques such as co-contraction has advanced to multiple DOFs, but only one DOF can be controlled at a time. Proportional control, in which the magnitude of EMG signal can be used to provide a gradient in movement speed and gripping force while operating was also implemented in these prostheses [9]. Though even after these advancements, prostheses are not in a stage that they can completely substitute the functionality of a normal human arm. Tasks such as reaching and picking up an object from the table that seems simple to a normal human arm are rather complex while achieving with a 'direct and proportionally controlled' prosthesis. It is because tasks like reaching and picking up an object require achieving movements in multiple DOFs smoothly, which is not available in these prostheses. Multiarticulate hands with direct and proportional control can achieve movements in multiple DOFs, but they utilize switching techniques for switching to different hand movements. This is neither intuitive nor a smooth motion [15].

On the other hand, PR based control with multiarticulate hands can provide an alternative to switching techniques. PR utilizes either classification or regression methods to decode a mapping between EMG signal features (such as EMG magnitude, mean, standard deviation, standard error of mean, etc.) and different hand movements (such as hand at rest, hand open, close hand, forearm pronation, fore-

arm supination, etc.), that allows for almost instantaneous switching between different hand movements [9]. This provided a sequential (one motion at a time) but smoother and a more intuitive control. But for a good PR based control, EMG patterns generated by the user should have specific feature qualities. For a reliable control, different EMG features should be consistent and reproducible across trials of the same hand movement and discriminative among different hand movements. To increase inter-class separability and intra-class consistency, user training is provided. In training the user learns and improves PR skills by practicing different hand movements repetitively with the help of visual feedback. As a result, users change control commands permanently in favour of those muscles they find easy to control [10] [15] [1]. With this, users can also develop their own strategies of control commands to make correct hand movements.

We know that training exercises help in learning to use a prosthesis, but we do not have an evidence based training program that can help us learn what we need to learn to be better at controlling prosthesis. Therefore, if we want to optimize learning, the first thing we should be able to answer is, ‘Learning what will change the activation of control commands to desired activations?’. We can answer this question only if we first will look for how the control commands change over learning. A similar study is performed in Franzke et al. (2020) to look for the changes in control commands. The PR based study addresses a significant improvement in online performance over training. To address the reason for the change, three EMG feature space metrics namely separability, variability, and repeatability were derived in the form of three parameters: separability index (SI), mean semi-principal axis (MSA) and repeatability index (RI), respectively. Changes in these parameters were tracked with respect to the offline and online performance over learning. But a strong significant correlation between these metrics and offline and online performance was not found except for the SI and offline accuracy. None of these parameters had a high predictive power with respect to online performance. Therefore, the reason for a significant increase in online performance could not get addressed with these EMG feature space metrics [16].

The change in control commands can also be addressed with the help of muscle synergies. Muscle synergies are defined as proportional activation of a group of muscles. A muscle synergy that is activated by a single neural command recruits the muscles in a group and activates them in a definite proportion to achieve a task [4][17]. Linear combinations of these synergies are capable of defining complex force and motion patterns in reduced dimensions [7]. We want to use this information of proportional activation of muscles with training exercises, to look for the changes in control commands over learning. This is the major goal of this study, which will answer how control commands change over learning. To understand the underlying mechanism for the change, EMG data of a training session will be decomposed into

two lower-dimensional subspaces, which, when linearly combined can explain for the originally recorded EMG data with high accuracy. These two subspaces are defined as muscle synergies and muscle activation coefficients. This is done by employing the non-negative matrix factorization (NMF) algorithm [18]. A change in any of these subspaces over learning can cause a permanent change in control commands. Therefore, two more research questions can be posed to understand the change in the underlying mechanism. Hence, the objective and research question of the study are:

Objective: How do control commands change over learning to use a pattern recognition (PR) controlled prosthesis.

Research Question 1: Do muscle synergies change over learning to use PR controlled prosthesis?

Research Question 2: Do muscle activation coefficient patterns change over learning to use PR controlled prosthesis?

Answering these questions will help us visualize a change in control commands over learning to use a PR controlled prosthesis and will help us to understand what users will need to learn to be able to develop certain control commands. These questions can be answered by performing a training exercise. In that, participants with normal upper limbs will learn to control a virtual prosthetic hand using a myoelectric controlled interface. Various hand movements such as hand at rest, hand open, close hand, index point, fine pinch, forearm pronation, forearm supination, wrist flexion, and wrist extension could be a part of this exercise [1]. To understand the change in control commands over learning, the virtual prosthesis should be controlled only by those sites which do that in a typical prosthesis. But to derive the synergies, EMG data should be acquired from all the muscles remaining in the upper limb in the case of a transradial amputation. This EMG data will be stored for further investigation. EMG data of each iteration of training exercise will be decomposed to find out muscle synergies and muscle activation coefficients [18]. Tracking the change in both these factors of EMG data will reveal what changes and what remains constant over learning. This will also help us to answer what needs to be learned by the user to get better with synergistic control and what should be avoided in learning to be able to generate required muscle synergies and control commands.

Due to the Coronavirus situation, the experiment planned could not take place. Therefore, we came up with a different solution to the problem. A dataset acquired for a different study, published in Kristoffersen et al. (2020) will be used in our study to derive the muscle synergies and muscle activation coefficients. The dataset consists EMG data of 20 participants, participated in a 5-day training exercise. A total of 15 training sessions each participant were recorded using eight electrodes

around the forearm [1].

In our previous plan, we wanted to record the EMG signals from multiple muscles in hand (approximately 20). But because now we have the EMG data of only 8 electrodes, the interpretation will differ, A lot more redundant information, which could have been able to define the muscle synergy structure will not be available. The information of only 8 electrodes will be used to look for changes in muscle synergies and activation coefficients. Because of the change in the data, the interpretation of results may differ, but the same aforementioned questions can be answered with this data.

Chapter 2

Materials and Methods

2.1 Participants

Twenty able-bodied participants took part in the study, of which 11 were females (mean age of the group = 22 ± 2.8 years). Participants were first asked to answer the handedness questionnaire of the Edinburgh inventory to assess their hand dominancy. Any neurological pathologies or musculoskeletal complaints interfering with study outcomes were part of exclusion criteria. All participants were informed about the experiment prior to the participation and were asked to sign a letter of consent. This study was approved by the ethical committee of the Department of Human Movement Sciences at the University Medical Center Groningen (UMCG). (ECB/2017.01.12_1) [1] [16].

2.2 Myoelectric machine learning system

Eight commercially available double differential electrodes (13E200=50 AC, Otto Bock Healthcare Products GmbH, Vienna, Austria) were used to acquire EMG signals. The electrodes were attached equidistantly around the thickest part of the non-dominant hand with help of a brace (Medical Specialties Wrist Lacer). Wrist and thumb movements were restricted. Participants were asked to produce isometric muscle contractions similar to those of a person with an upper limb amputation. The EMG signal outcomes from the electrodes were pre-amplified and band-pass filtered. EMG data were sampled at 1000 Hz and transmitted to a laptop computer wirelessly via Bluetooth connection. The software used to record EMG data was provided by Otto Bock Healthcare Products GmbH (Vienna, Austria). It was also used to train a classifier, and to run a match-prompt test for measuring the online performance [1] [16].

2.3 Procedure

The learning experiment was conducted over 5 days as a daily training exercise. On day 1, a pre-test of \approx 10 minutes was performed followed by a 20-minute user training session. On days 2-4, participants performed a 30-minute user training session. On day 5, participants performed a 20-minute user training session followed by a post-test that lasted for \approx 10 minutes.

Pre and post tests were identical and comprised of two parts: System training and Motion Test. In system training various hand movements were performed for a training session and the EMG data was used to train a model to construct a feature space using linear-discriminant-analysis (LDA) classifier. Eight hand movements: rest, wrist supination, wrist pronation, wrist flexion, wrist extension, hand open, fine pinch grip, and lateral thumb grip were part of the training exercise. After the classifier model training, a match prompt test was performed, in which the software instructed the participants to perform different hand movements randomly. The performance was assessed with number of correct hand movements. Data of all tests and training sessions were stored for further computations [1] [16].

2.4 The dataset

Each of the 20 participants performed 15 training sessions (except for participant 8, 12th training session was not performed). Participants were asked to perform eight hand movements, each for three seconds. This exercise was performed three times for the prompted levels of 30% maximum volumetric contraction (MVC), 60% MVC and 90% MVC. Therefore, total 24 hand movements make a muscle matrix for a single learning session [1] [16].

2.5 Data Analysis

Matlab R2018a from The MathWorks, Inc. was used for all type of data analysis and plotting. Before working on data to find muscle synergies and activation coefficients, it was pre-processed to fit any mathematical model [19].

2.5.1 Pre-processing

Each training session consists of different hand movements at different MVC levels. Before applying any pre-processing technique, all the data from a single training

session is required to permute in a single 2-D matrix [18]. Therefore, raw EMG data of 8 electrodes for different hand movements of a training session were stacked together to make a muscle matrix as shown in equation 2.1.

$$M(\theta) = \begin{matrix} \text{muscle 1} \rightarrow & \left[\begin{matrix} m_1(\theta_1) & m_1(\theta_2) & \cdots & m_1(\theta_{24}) \end{matrix} \right] \\ \text{muscle 2} \rightarrow & \left[\begin{matrix} m_2(\theta_1) & m_2(\theta_2) & \cdots & m_2(\theta_{24}) \end{matrix} \right] \\ \vdots & \left[\begin{matrix} \vdots & \vdots & \ddots & \vdots \end{matrix} \right] \\ \text{muscle 8} \rightarrow & \left[\begin{matrix} m_8(\theta_1) & m_8(\theta_2) & \cdots & m_8(\theta_{24}) \end{matrix} \right] \end{matrix} \quad (2.1)$$

To extract non-negative lower dimensional subspaces of this muscle matrix via NMF algorithm, the input data matrix should be non-negative. Hence, absolute value of each data point was calculated to get a non-negative EMG envelope . To match the activity level in all electrodes, the values in each row (electrode) were normalized to the maximum level of muscle activity observed for that muscle across all conditions. Normalization also helps in better fitting any mathematical model to the data [6][20] [18].

2.5.2 Muscle synergies' model and NMF

NMF is a linear decomposition technique that assumes that the input data is composed of linear combinations of lower dimensional underlying elements. Therefore, if provided a number of simultaneous observations through multiple channels, an observation data can be represented as:

$$M_j = h_{1j}W_1 + h_{2j}W_2 + \cdots + h_{nj}W_n + error \quad (2.2)$$

Here, on the left side of the equation M_j is a matrix that represents measurements of multiple EMG channels. Given, if a muscle matrix is of size $[m, n]$, represents that m channels were recorded for n number of observations. On the right side are the components or basis vectors W_i , are vectors of length m . They represent invariant patterns of activity across those different channels. The ‘coefficients of muscle activation’ are described by n scalar values h_{ij} , each of its value specifies the contribution of each basis vector to the measured muscle activation pattern M_j . If there are m muscles and $k < m$ basis vectors, it means that W_i and h_{ij} are lower-dimensional than M_j . Therefore, linear decomposition techniques hypothesize that, if number of observations of M_j are large, keeping the components W_i fixed, and scaling factors h_{ij} allowed to change, when combined, can sufficiently account for all the variation in the observed data [18]. These fixed basis vectors of muscle activation patterns are also termed as ‘fixed muscle synergies’ [18][12][4].

NMF is also comprised of the same aforementioned hypothesis. In it, lower dimensional subspaces of the input data are found using a search algorithm. Therefore, the

solution starts with random W and h initial values (if not specified specifically). It linearly combines basis vectors and activation coefficients of these random matrices and calculates the error between observed and reconstructed data . In further iterations it updates W and h matrices based on different error minimization techniques. One of them is multiplicative update rule, which was used in this study [18] [21]. NMF is constrained to decompose the data into non-negative components, therefore, the problem NMF deals with is generally called *convex*. There are no local minima in this type of search. Hence, approximately nearby solutions are achieved. It means that basis vectors and activation coefficient patterns will not be numerically same but will be very similar. Also, in a non- negative space it is not possible that the components can be orthogonal. Therefore, the basis vectors are independent. It means that vector(s) itself as well as their linear combinations can not define any of the other vector(s). NMF also adapts for the physiological similarity of neural and muscle output. Muscle activations are a resultant of neuron firing. Since neurons are either firing action potentials (positive value) or else are in resting state (zero value), resembles that the muscle activation data should be non-negative. That makes NMF one of the algorithms that can decompose the muscle activation data with very high accuracy [18].

$$m(t) = \sum_{i=1}^k h_i(t)w_i + \text{error} \quad (2.3)$$

$$\begin{bmatrix} M \\ \end{bmatrix}_{m*n} = \begin{bmatrix} W \\ \end{bmatrix}_{m*k} \begin{bmatrix} H \\ \end{bmatrix}_{k*n} + \text{error} \quad (2.4)$$

In fixed muscle synergy approach using NMF, if $k < m$ muscle synergies are extracted, the dimension of muscle synergy matrix will be $[m,k]$, and the dimension of muscle activation coefficients matrix will be $[k,m]$. It can also be written as equations 2.3 and 2.4:

2.5.3 Muscle synergy extraction criteria

2.5.3.1 Dimensionality analysis

For the extraction of muscle synergies, we can define the number of basis vectors we want to extract using NMF. It simply means that the data will be a linear combination of that many components and activation coefficient patterns. For an 8-muscle observation data ‘ $k=1-8$ ’ number of basis vectors can get extracted. To find the optimal number of basis vectors, variance explained for (VAF) of the reconstructed data with respect to the original data was calculated for 1-8 basis vectors [6] [20] [22]. Calculation for each 1-8 numbers of basis vectors was iterated for 50 times with

random initial values for W and H. Out of each set those solutions were stored that provide maximum VAF for that group of solutions. This was done to increase the possibility of finding a solution that can give a global minima of error [6]. Apart from VAF, squared Pearson's correlation coefficient (R^2) was also calculated to find the measure of the strength of a linear association of observed and reconstructed data [18]. VAF was kept as main parameter for selection of the solution, was computed as per equation 2.5.

$$\text{VAF} = 1 - \frac{\text{SSE}}{\text{SST}} \quad (2.5)$$

Here, SSE is the sum of squared errors of the reconstructed data by multiplying W and H matrices, and SST is the sum of squared residuals of the observed data with respect to the mean of that row of matrix M_j . R^2 was calculated using the 'corr2' function of Matlab.

2.5.4 Simulated data: Is 8-channel data enough to apply NMF?

In our previous plan we wanted to record the EMG data from a large number of muscles. But because now we are using an 8-channel recorded data, we want to be sure if the NMF can be applied to only an 8-channel muscle matrix data and can still be able to produce very similar solutions (i.e. approximate solutions to the global minima). For that we generated a 22-channel and an 8-channel per-muscle-normally-distributed muscle data. Number of observations were similar to as of the original recorded data. The simulated data were generated as a weighted combination of basis vectors as shown in equation 2.6.

$$\vec{d} = g\left(\sum_{i=1}^k h_i \vec{w}_i + \text{error}\right) \quad (2.6)$$

Here, \vec{d} is an m dimensional data vector, which is enforced to be non-negative by a threshold function $g(\vec{x})$. The non-negativity is constrained by making negative values zero, such that $y_i = 0$ for $x_i < 0$ and $y_i = x_i$ for $x_i \geq 0$ [23].

To verify if the spread in this data is similar to our original observed data, histograms were plotted of the simulated and observed data. Distribution of different values in different bins were observed. Bins represent intervals, and individual values are stacked in the intervals they belong to. If the distributions are similar, inferences from the analysis of simulated data can be applied to the observed data [24].

Further, after the verification of similarity in distribution, NMF will be applied

to both data. If the outcomes of muscle synergy and activation coefficient matrices remain stable for both 8-channel and 22-channel simulated data, it will be concluded that an 8-channel simulated data is good enough to apply NMF to it. Additionally, if the distribution of an 8-channel observed data is similar to an 8-channel simulated data, NMF can be applied to the observed data too.

2.5.5 Simple vs Forced solutions via NMF

NMF can be applied in two ways. First being the default ‘nnmf’ of Matlab with default options, and second is a modified form of NMF. The default ‘nnmf’ will be used first [25]. But if the outcomes will not be stable, the modified form will be used. It will force to minimize the global error over large number of iterations [26] [21]. Therefore, it will help in reaching similar solutions. The only problem with forced solutions is that, it requires more computation power. Therefore, default options will be tried out first.

2.5.6 Similarity analysis

In this study, we are applying NMF to the muscle data to find out muscle synergies and activation coefficients. For that we stacked all the muscle synergies one below another based on their training session numbering. This will help us track a change in muscle synergy structure from training session-1 to training session-15 for all participants. Similarly, this procedure will be applied on activation coefficient patterns too. But, because the NMF solver can produce the same solution by shuffling the basis vector column positions, it is required to match the solutions in a pair-wise manner, where all basis vectors of the following training session are matched with the basis vectors of previous training session solution. Based on the best match of basis vectors, they are shuffled and the solutions are rearranged. This is done to match the synergy structures of all training sessions. It makes sure that change in the same basis vector is being tracked over the training sessions [6] [22] [20]. When we plot the sorted solutions, we can see how activations in muscles synergies and muscle activation coefficient patterns are changing over learning.

There were four strategies used to match muscle synergies [6]. They are, i) Visual inspection ii) normalized dot product (NDP) [27] iii) cosine of principal angles (CPA) [28], and iv) k-means clustering [29].

In visual inspection bar graphs of muscle synergies are plotted. Based on matching the activations visually, a trend can be defined, but sometimes it is relatively tough. Therefore, mathematical operations were preferred for matching muscle synergies. They are NDP and CPA. NDP and CPA used pair-wise calculations for matching.

‘dot’ and ‘subspace’ of Matlab were used to find out NDP and CPA, respectively. Based on NDP and CPA two different sorted solutions were developed for basis vector matching.

K-means clustering is a technique to find out group similarity. It breaks the data into k numbers of clusters [29], therefore, if $k=4$ numbers of synergy structures can be clustered, it can provide us a group matching of synergies. For that, for each participant clustering was done by pooling all basis vectors and finding out four clusters of them using the ‘cosine distance’ between basis vectors as a metric [6]. This provided the third solution for tracking the change in structure of muscle synergies.

We are also interested in average initial and average final behaviour of muscle synergies and activation coefficient patterns after training. Therefore, we averaged muscle synergies of 5 initial and 5 final training sessions after matching them with k-means clustering into four clusters of equal size. Averaging the clustered solutions provided initial and final averaged behaviour of muscle synergies. A measure of average initial to final change in muscle synergies was calculated with CPA, which denotes an angular change in the structure of each muscle synergy.

Clustering for muscle activation coefficient patterns was not performed separately. Muscle activation patterns were also matched based on the clustering of muscle synergies. Their averaged initial and final behaviours were also computed. Activation coefficients are scalar quantities that denote the level of activation over observed variations in individual muscle synergies [18] [23]. Therefore, calculating CPA for scalar quantities is mathematically wrong. Henceforth, to showcase a change in initial and final averaged activation coefficient patterns’ structure, mean with its standard deviation (SD) was calculated for both solutions. A quantitative change in mean and SD will indicate that muscle activation patterns also change. But moreover it denotes that activation level over different activities is changing, which is also possible if different hand movements were performed with slightly different MVC. Therefore, activation coefficients are much sensitive and dependent on activity type and MVC used in the activity.

For a good outcome, the results of NDP, CPA and k-means clustering should show a matching of same basis vectors and activation coefficient patterns over different training sessions. And, k-means clustering should cluster the synergies in four equal clusters.

Chapter 3

Results

3.1 Dimensionality analysis

Eight solutions of 1-8 basis vectors were calculated based on the best VAF out of 50 iterations of each training session data. For our data, on an average 3 basis vectors can explain for 69.89% data. If we consider a 4 basis vector solution, there is a jump of 9.67%, and that makes the average VAF 79.57%. Likewise, VAF and its cumulative difference are mentioned in table 3.1. In literature, we found that the cumulative difference of VAF decreases drastically if 4 basis vectors are extracted instead of 3, and so on for more number of basis vectors [6] [20]. Therefore, if the cumulative difference of VAF is much lesser, 3 muscle synergies can explain for almost the same data as much as that of 4 basis vectors. In Muceli et al. (2014), for a 16-channel configuration, the cumulative difference between a 2 basis vector solution and a 3 basis vector solution is just $\approx 2\%$. More than 3 vectors make only a little difference. Hence, 3 number of optimum basis vectors were chosen [20]. In our data, this cumulative difference is much bigger for every solution.

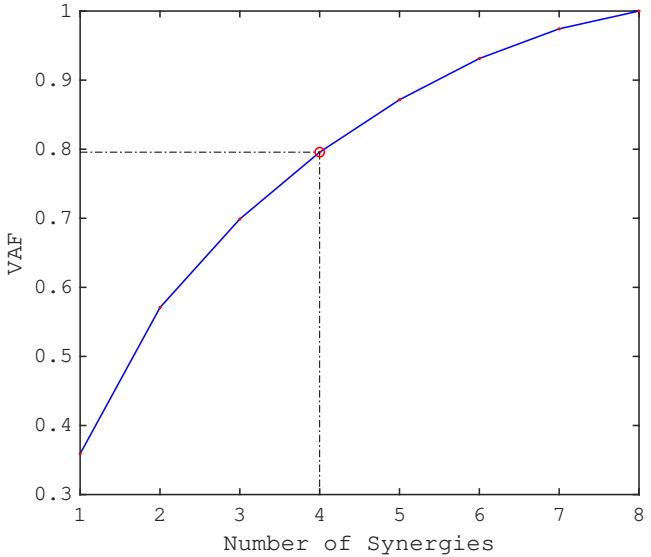


Figure 3.1: Graphical representation of muscle synergy extraction: variance explained for (VAF) versus number of synergies (k)

Therefore, an optimal number of basis vectors can not be chosen by seeing the cumulative difference. Hence, because 4 basis vectors can explain for as good as 80% variance in the data, it was chosen as the dimension of basis vectors. Values of maximum VAF vs k are plotted in figure 3.1.

Table 3.1: Number of synergies vs VAF and its cumulative difference

Number of Synergies	VAF (%)	Cumulative Difference (%)
1	35.91	
2	57.08	21.16
3	69.89	12.81
4	79.57	9.67
5	87.16	7.59
6	93.13	5.96
7	97.43	4.29
8	100	2.57

3.2 Simulated data vs Observed data

After selecting four numbers of basis vectors as the dimensionality of the muscle synergy solution, a 22-channel simulated data, an 8-channel simulated data, and an 8-channel observed data were compared to find out the distribution of different values in the simulated and observed data. We found out that the spread over bins in both cases is similar for low level of activation. But, there were lesser values in bins of high level of activation. It can be seen in figure 3.2. There is some difference in the distribution of data, so that, behaviour of both data may differ.

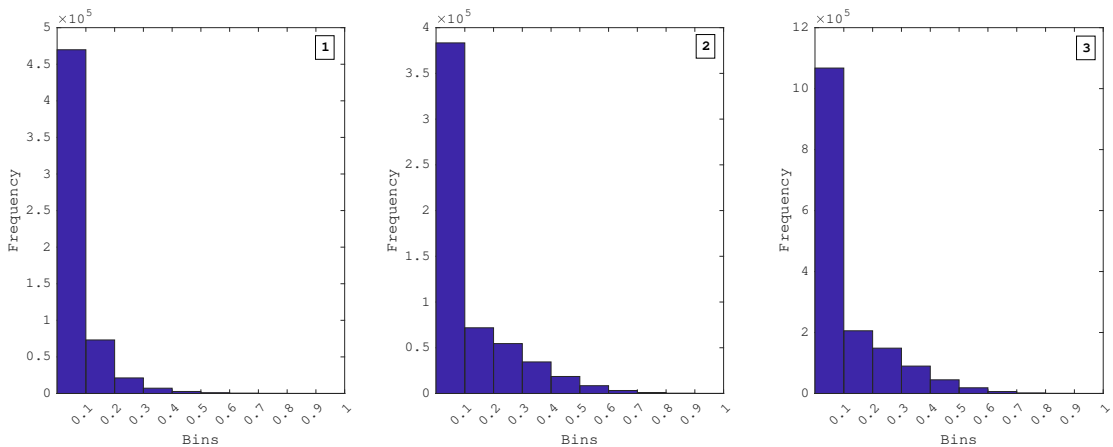


Figure 3.2: Histograms of (1) an 8-channel observed data, (2) an 8-channel simulated data, and (3) a 22-channel simulated data

Further, Firstly, we worked with ‘nnmf’, the default NMF algortihm of Matlab with default options (algorithm: als, MaxIter:100, TolX:1e-4, TolFun:1e-4) [25]. The solutions achieved using this data were showcasing VAF of approximately 65% for an 8-channel simulated data and approximately 25% for a 22-channel simulated data. When calculated the solutions for the same data repetitively, a correlation of 84.04% for the 8-channel data and 36.83% for the 22-channel data was found out. It means that the solutions are not reaching to the global minima of error. To be able to track changes in muscle synergy and activation command structure, it is important that achieved solutions should be stable and show high ($\geq 80\%$) correlation to a re-iterated solution. A high VAF ($\geq 80\%$) also ensures that information in input data and processed outcomes is highly relevant. So that, our solutions should showcase both these properties to be able to track changes in muscle synergies and activation commands. While comparing solutions, it was also observed that basis vector and activation matrix can shuffle the columns and rows for same solution, respectively. Therefore, related columns are required to match with previous solution to find the correlation between solutions [6][22][20].

Further, in search of the solution related to the global minima of the error, we force calculated them using a customized NMF algorithm [30]. The solver starts with random initial W and H matrices, and over iterations tries to minimize the error between provided data and solution regenerated data [30][26][21]. To be sure if the global minima is reaching, repeated calculations were done with different number of iterations with different initial W and H matrices. A correlation of 100% was found out for repeated solutions of both simulated data. This ensured that NMF is capable of producing exact as well as very approximate solutions if provided data has a unique solution. A loop ‘break’ condition that if the mean absolute percentage error goes below 10^{-5} aborts the loop and consider that outcome as final solution was also implemented to provide an accuracy cut-off to the solution [30]. This condition was not met for both simulated data, yet after 10,000 and 25,000 iterations both data show same results repetitively, respectfully. This made sure that solutions are not iteration dependent and are actually related to that of the global minima.

In literature we also found that the number of channels do not influence the structure of basis vectors or the shape of activation signals. In Muceli et al. (2014) it was confirmed that when using 6, 8, 16 or as many as 192 channels, it will not affect the structure of the solution [20]. Therefore, in our proposition, an 8-channel dataset having a large number of observations can be used with NMF, and muscle synergies and activation coefficients can be extracted from our data.

3.2.1 Simple vs Forced solutions via NMF

In the previous subsection we worked on simulated data. With forced solution we were able to get recurring solutions for simulated data. But, when working with observed data and forced solutions, more than one results were obtained for the same data. Therefore, four solutions were calculated while working with original observed data. First with default ‘nnmf’ of Matlab [25] and rest three with customized NMF algorithm with 10,000, 25,000 and 50,000 iterations [30]. Multiple solutions were calculated to make sure if global minima of error is reaching or at-least nearby solutions with a high correlation ($\geq 80\%$) are achieved. The solutions are named as following:

1. Muscle Synergy and Activation Coefficient sub-spaces with ‘nnmf’ and best VAF of 50 solutions: Wb50 and Hb50
2. Muscle Synergy and Activation Coefficient sub-spaces with custom NMF after 10,000 iterations: W10 and H10
3. Muscle Synergy and Activation Coefficient sub-spaces with custom NMF after 25,000 iterations: W25 and H25
4. Muscle Synergy and Activation Coefficient sub-spaces with custom NMF after 50,000 iterations: W50 and H50

Furthermore, we compared these four solutions participant and training session number wise. We matched the solution matrices in a pair-wise manner and found out the best match of basis vectors based on Normalized Dot Product (NDP) [6]. We found out that some solutions of W10 and W25 were not similar, this gave the idea that maybe the minima was not reached, therefore, we expected it to reach with the W50 solution. Yet, some of the W50 solutions that were not same as of W25, were similar to W10. This gave the idea that more than one solutions were achieved, which was dependent on either the initial condition or the number of iterations. If we consider the hypothesis that after a large number of iterations, a solution that is achieved at-least twice (same or similar) of W10, W25, W50 and Wb50 is the global solution for that particular training session’s muscle matrix, there was such a solution available for each participant’s each training session. Based on this hypothesis a new solution was developed that contains only those solutions, are related to the global minima of error.

Further, We will use this solution to track changes in the muscle synergies and activation coefficients over learning in different training sessions.

3.3 Similarity analysis

Similarity analysis was performed on the calculated solution to match related muscle synergies over training sessions for each participant. Synergy matching was based on NDP, CPA and K-means clustering [27][28][29][6].

3.3.1 *NDP and CPA*

Matching with NDP and CPA follows a procedure that compares basis vectors of second training session with basis vectors of first training session in a pair-wise manner. Based on highest combination of NDP (or lowest with CPA), basis vectors of second training session are shuffled. Likewise, the n^{th} session is matched with shuffled solution of $(n - 1)^{th}$ session [6]. This procedure follows up to the fifteenth training session. With NDP and CPA matching, same matching results of muscle synergies were obtained for each participant.

When visually inspect the results with bar graphs, traces of mismatch can be noticed. It happens because we are working with only 8-muscle's activation data, which seems to be less number of muscles to keep tracking the formation of activations in muscle synergies. Also, because the combination of different activations in each basis vector can produce higher or lower NDPs or CPAs, respectively, which can lead to a different pair matching.

An example of the results obtained via. NDP and CPA analysis can be seen in figure 3.3. Here, for participant 9 (P9), 2nd and 4th synergies (W_2 and W_4) are mismatched after training session 6. This happened because in training sessions 4,5, and 6 the participant tried using muscle-6 much more actively rather than muscle-5 in synergy W_2 , and as after training session 6, when muscle-5 was preferred to use again instead of muscle-6, the structure matching got changed, and W_4 from there got shifted to W_2 because NDP of a that match was higher (or CPA was lower). Similar and more complex mismatches in muscle synergy structure can be witnessed for other participants too. Those plots are included in Appendix.

Similarly, the change in activation coefficients was also tracked, but the basis of activation coefficients' matching is also the similarity in muscle synergies. To do that, activation coefficients were also shuffled row-wise as basis vectors were being shuffled column-wise. This matrix operation makes sure that correct basis vectors and activation coefficients are getting linearly combined to reconstruct the original data. Because activation coefficient has large data-points, to visualize them clearly in form of curves, it was first down-sampled by a factor of 100 and later filtered through a 3rd order butterworth filter with a half power frequency of 0.2 [31].

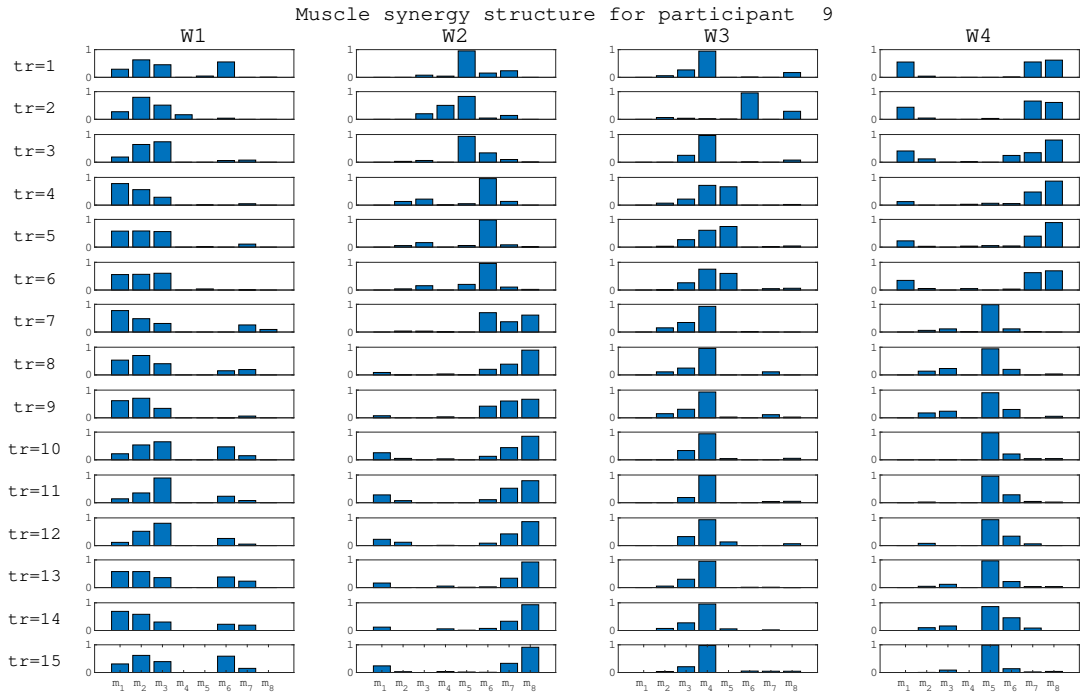


Figure 3.3: Bar-graphs of four muscle synergies (W1-W4) over training sessions (tr) for participant 9, matching is done by NDP (or CPA), m_1 to m_8 on x-axis represent 8-muscles, bars show the fixed muscle synergy activations of muscles

For P9, the change in activation coefficients can be seen in figure 3.4. Mismatches in figure 3.3 and figure 3.4 are same. As in figure 3.4 change in W_1 and W_3 can be seen following a trend, similarly, a trend of change in activation coefficients pattern can be seen in H_1 and H_3 . The mismatch of H_2 and H_4 can also be noticed after training session-6. Activation coefficients' plots for other participants are also included in Appendix.

It is also important to notice that change in muscle synergy structure is happening after each training session. If these changes are small in terms of level of activation, and different muscles are not being used, NDP and CPA can track the change in a mechanised manner. But because the change is not that uniform, clustering our muscle synergy solutions into four clusters can help us matching the synergies.

3.3.2 *k-means Clustering*

Clustering by k-means is an advanced method for matching the basis vectors [29]. For each participant, synergies were pooled and clustered into four groups. Each group should consist 15 synergies if synergies were grouped properly by k-means. But because there exist solutions, in which basis vectors of same training session

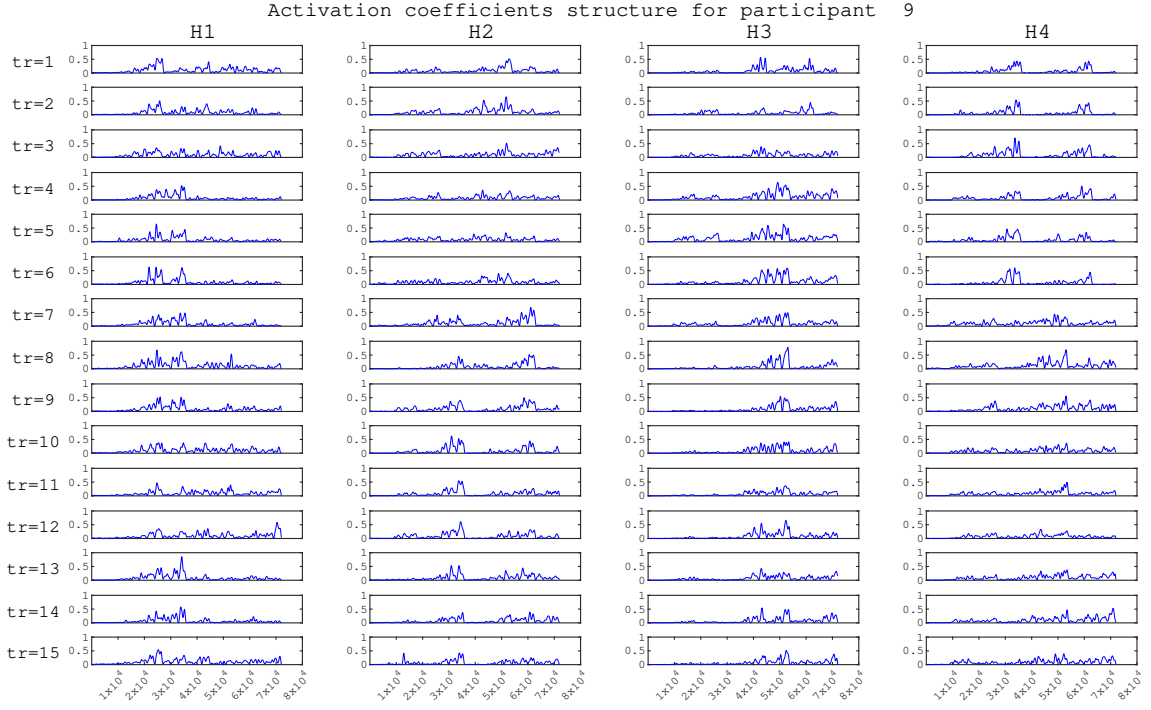


Figure 3.4: Change in four activation coefficient patterns (H1-H4) over training sessions (tr) for participant 9, matching is adopted from the matching of related muscle synergies, X-axis represents number of total observed points

show more similarity than any of other muscle synergies, hence, the sizes of clusters are not equal to 15 for most of the participants. Only for P3 and P19 proper clustering was achieved. Clustering size for each participant is shown in the table 3.2.

From the table it can be noticed if the minimum cluster size is of 13 and maximum of 17, 14 participants fall in that range. For them, the mismatch exist only for 0-2 muscle synergies. For the rest 6 participants more synergies are falling in other clusters.

With clustering the change in muscle synergies is presented in the form of spider plots [32]. It gives a representation of activations in the arm muscles. An example of spider plot is presented in figure 3.5. Here, from center to vertical top axis represents activation in 1^{st} muscle (m1). The activation scales are marked on the axes. Likewise, adjacent axis in the clockwise direction is 2^{nd} muscle (m2) and adjacent axis in the anti-clockwise direction is 8^{th} muscle (m8). The activations in four different muscle synergies are shown in four colours. We can see that the first (blue), second (red), third (yellow) and fourth (violet) muscle synergies are dominant in different muscles i.e m4, m1, m5 and m6, respectively.

When training is provided, the activations in muscles may change. That lead to a change in the synergy structure. As a resultant, either a different muscle or a different level of activation in the same muscle is used to control the same task.

Table 3.2: Cluster size for each participant by k-means

Participant (P#)	size Cl 1	size Cl 2	size Cl 3	size Cl 4
1	15	15	13	17
2	16	13	16	15
3	15	15	15	15
4	14	11	20	15
5	16	15	14	15
6	13	16	16	15
7	14	15	17	14
8	14	14	15	13
9	15	14	15	16
10	16	18	12	14
11	19	12	15	14
12	16	13	15	16
13	16	14	14	16
14	14	16	15	15
15	15	15	17	13
16	15	18	15	12
17	18	13	15	14
18	15	17	14	14
19	15	15	15	15
20	18	12	19	11

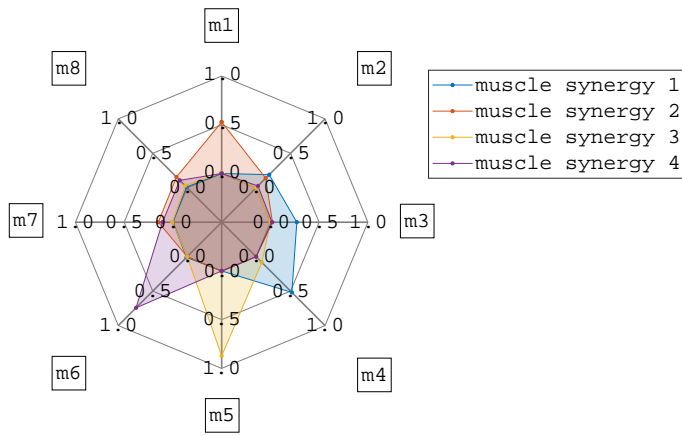


Figure 3.5: Graphical representation of muscle synergy structure: four different colors show four muscle synergy structures and the activation scales are mentioned on the axes.

For P3 and P19 from training session-1 to training session-15 the change in muscle synergy structure can be visualized in figures 3.6 and 3.7, respectively. Initially for P3 the first (blue), second (red), third (yellow), and fourth (violet) muscle synergies are dominant in muscles m4, m1, m5, and m6, respectively, after the first training session. But, after the fifteenth training session dominant activations change to muscles m5, m1, m7, and m8, respectively. Similar changes can also be noticed for P19. Activation coefficient patterns' matching is also done for P3 and P19, which is also based on the clustering of muscle synergies. Their plots are represented in figure 3.8 and 3.9, respectively.

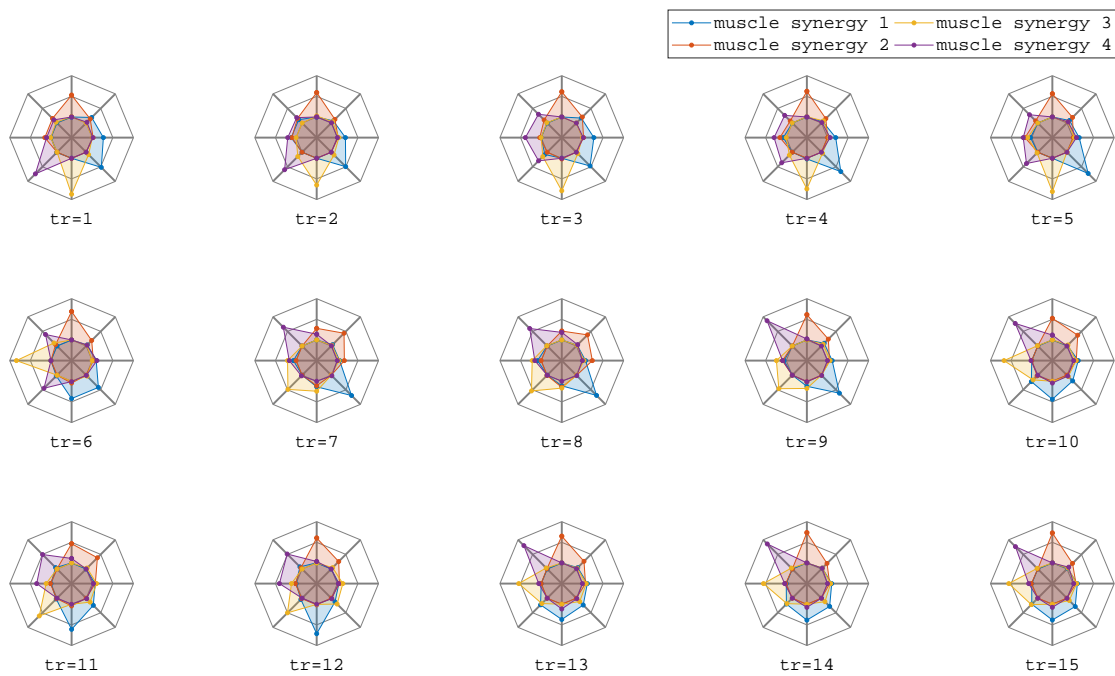


Figure 3.6: Spider plot for P3: different colors show the different synergies (W1-W4). Top (training session 1-5), mid (training session 6-10) and bottom (training session 11-15). A change in the muscle synergy activation and distribution can be noticed from training session 1 to training session 15. Matching is done by k-means clustering.

Plotting other solutions in spider plot is relatively tough. It is because the size of four muscle synergy clusters are not equal for every participant. Plotting muscle synergy solutions in bar graphs showcases that distribution of activations within a few initial and a few final training sessions remains similar. Therefore, averaging a few initial and a few final synergies can give us the idea that how initial and final behaviour is after training. Clustering a few synergies into four equal groups will be relatively easy too because structure of muscle synergies do not change drastically in initial and final few training sessions. This was implemented for 5 initial and 5 final solutions. Proper clustering for four participants (P6, P7, P8 and P19) in initial training sessions and three participants (P6, P17 and P18) in final training

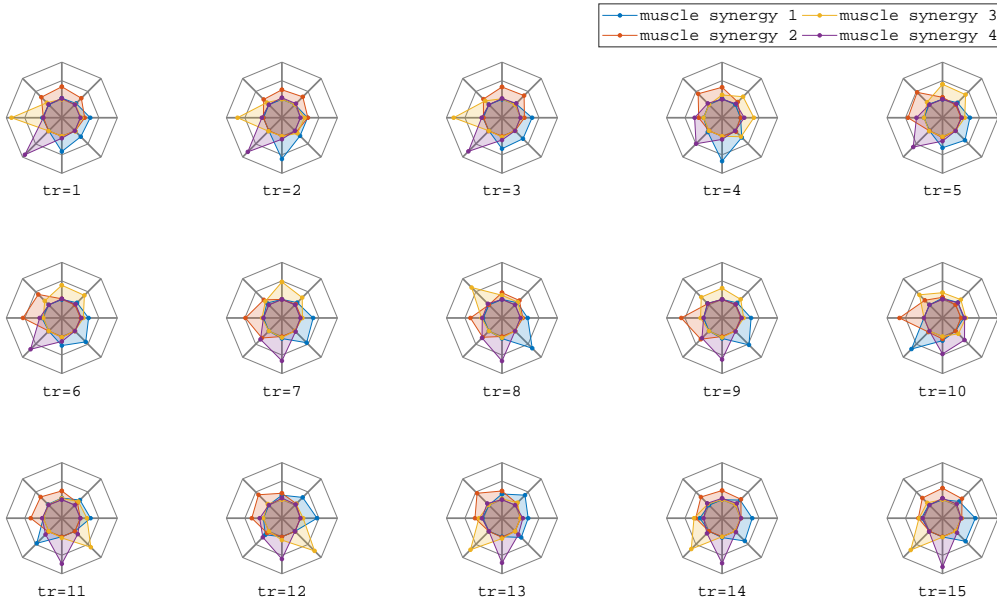


Figure 3.7: Spider plot for P19: different colors show the different synergies (W1-W4). Top (training session 1-5), mid (training session 6-10) and bottom (training session 11-15). A change in the muscle synergy activation and distribution can be noticed from training session 1 to training session 15. Matching is done by k-means clustering.

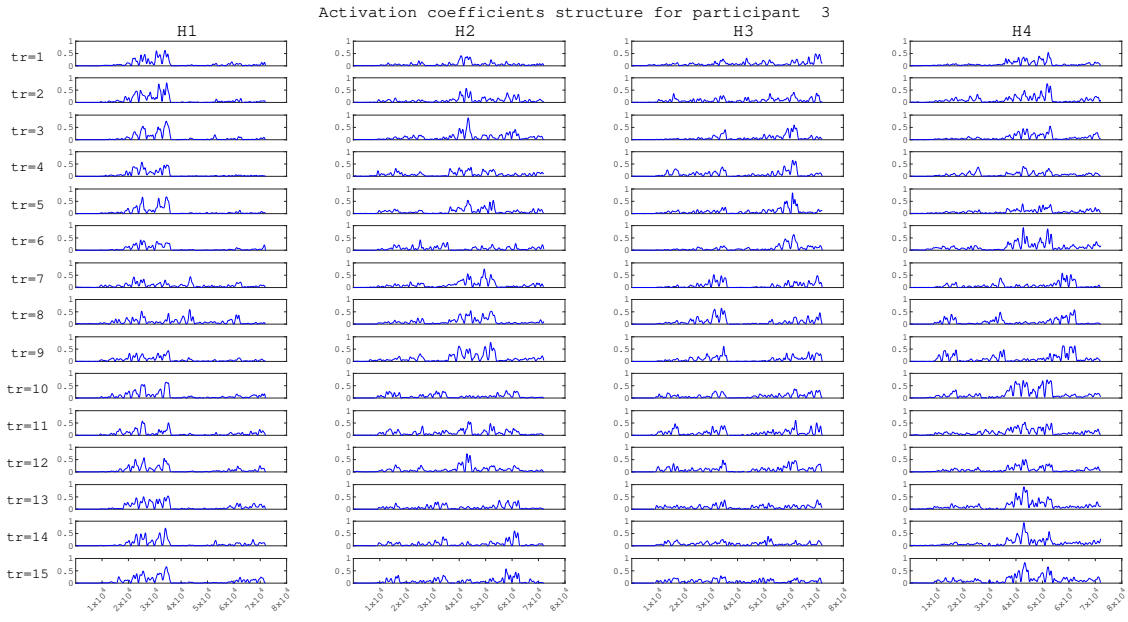


Figure 3.8: Change in four activation coefficient patterns (H1-H4) over training sessions (tr) for participant 3, matching is done by k-means clustering of muscle synergies

sessions could not be achieved. The maximum mismatch was of 1 synergy. Yet, because of this mismatch the averaged outcomes will change, but the averaging was done as per the clusters were acquired. After averaging the solutions, CPA was

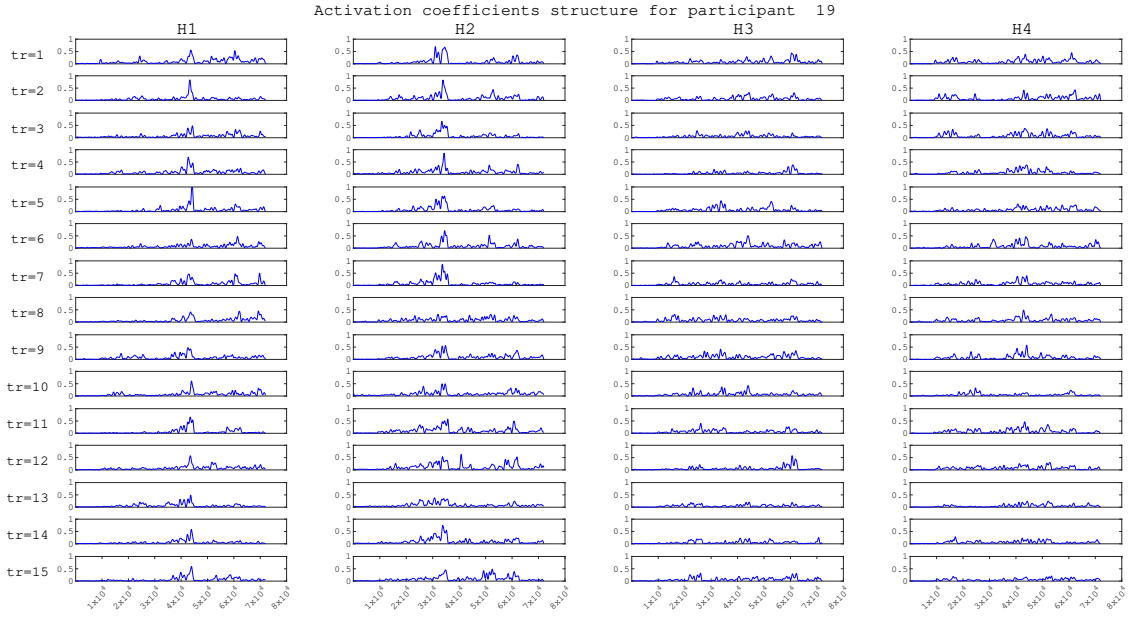


Figure 3.9: Change in four activation coefficient patterns (H1-H4) over training sessions (tr) for participant 19, matching is done by k-means clustering of muscle synergies

calculated between initial and final muscle synergies. The CPA value denotes the angular change in muscle synergy vectors. The value ranges from 0 to $\pi/2$ [33]. The angular change in synergy structure for all the participants is mentioned in table 3.3.

The change in initial and final averaged muscle activation coefficient patterns were also calculated. Variations in muscle activation coefficient patterns are represented in form of mean \pm SD for each coefficient array. This gives the idea of mean level of activation over different hand movements and a range of its change. If mean and SD change from initial to final averaged solutions, it means that different activities are taking place with different level of activations after training. Mean with SD for initial and final averaged solutions is shown in table 3.4.

Table 3.3: From initial to final averaged solution, angular change (CPA) in synergy structure for each participant

(P#)	W1	W2	W3	W4
1	0.16	0.09	0.59	0.38
2	0.75	0.97	1.47	1.43
3	1.43	0.69	1.47	0.22
4	1.36	1.48	0.81	1.50
5	1.28	1.38	1.43	1.28
6	1.47	1.51	0.97	1.25
7	1.45	1.49	0.09	1.36
8	1.39	1.43	1.41	1.20
9	0.21	0.12	0.14	0.25
10	0.53	1.48	1.48	0.18
11	0.81	1.25	1.01	0.14
12	1.48	0.18	1.39	1.38
13	0.25	0.71	0.42	0.56
14	0.28	0.34	0.24	0.34
15	0.14	0.10	0.68	0.95
16	0.94	0.13	0.58	1.43
17	1.39	1.34	0.32	1.34
18	1.15	1.45	1.51	0.07
19	1.35	1.28	0.93	0.50
20	1.45	0.08	1.33	1.48

Table 3.4: Initial and final averaged solutions of activation coefficient patterns, represented in form of mean \pm SD for each participant

(P#)	Initial averaged act. coefficient pattern (mean \pm SD)				Final averaged act. coefficient pattern			
	H1	H2	H3	H4	H1	H2	H3	H4
1	0.064 \pm 0.056	0.064 \pm 0.067	0.079 \pm 0.055	0.066 \pm 0.073	0.058 \pm 0.061	0.054 \pm 0.074	0.079 \pm 0.057	0.063 \pm 0.071
2	0.072 \pm 0.100	0.088 \pm 0.089	0.065 \pm 0.059	0.080 \pm 0.084	0.072 \pm 0.070	0.069 \pm 0.069	0.063 \pm 0.10	0.065 \pm 0.062
3	0.079 \pm 0.100	0.087 \pm 0.072	0.083 \pm 0.078	0.105 \pm 0.092	0.087 \pm 0.097	0.085 \pm 0.091	0.080 \pm 0.14	0.084 \pm 0.09
4	0.083 \pm 0.067	0.065 \pm 0.076	0.084 \pm 0.051	0.068 \pm 0.052	0.085 \pm 0.065	0.071 \pm 0.087	0.090 \pm 0.065	0.066 \pm 0.063
5	0.010 \pm 0.082	0.093 \pm 0.074	0.090 \pm 0.062	0.112 \pm 0.074	0.104 \pm 0.081	0.098 \pm 0.091	0.090 \pm 0.076	0.099 \pm 0.086
6	0.074 \pm 0.072	0.060 \pm 0.066	0.076 \pm 0.060	0.068 \pm 0.065	0.079 \pm 0.072	0.078 \pm 0.072	0.054 \pm 0.059	0.066 \pm 0.067
7	0.075 \pm 0.052	0.076 \pm 0.061	0.084 \pm 0.068	0.056 \pm 0.066	0.067 \pm 0.060	0.097 \pm 0.086	0.073 \pm 0.068	0.067 \pm 0.059
8	0.095 \pm 0.076	0.094 \pm 0.062	0.110 \pm 0.072	0.083 \pm 0.057	0.081 \pm 0.077	0.095 \pm 0.072	0.084 \pm 0.076	0.083 \pm 0.064
9	0.093 \pm 0.082	0.085 \pm 0.088	0.079 \pm 0.090	0.091 \pm 0.071	0.089 \pm 0.089	0.092 \pm 0.091	0.089 \pm 0.082	0.072 \pm 0.099
10	0.080 \pm 0.085	0.086 \pm 0.065	0.078 \pm 0.078	0.077 \pm 0.071	0.078 \pm 0.074	0.059 \pm 0.068	0.097 \pm 0.088	0.063 \pm 0.065
11	0.080 \pm 0.067	0.065 \pm 0.069	0.101 \pm 0.084	0.096 \pm 0.127	0.066 \pm 0.059	0.099 \pm 0.096	0.096 \pm 0.132	0.076 \pm 0.067
12	0.081 \pm 0.042	0.092 \pm 0.055	0.083 \pm 0.064	0.104 \pm 0.078	0.085 \pm 0.051	0.094 \pm 0.056	0.089 \pm 0.070	0.096 \pm 0.066
13	0.077 \pm 0.078	0.080 \pm 0.078	0.079 \pm 0.070	0.079 \pm 0.076	0.067 \pm 0.076	0.067 \pm 0.078	0.059 \pm 0.051	0.067 \pm 0.075
14	0.081 \pm 0.056	0.097 \pm 0.085	0.083 \pm 0.087	0.091 \pm 0.068	0.084 \pm 0.068	0.097 \pm 0.085	0.067 \pm 0.067	0.089 \pm 0.084
15	0.064 \pm 0.078	0.080 \pm 0.071	0.072 \pm 0.096	0.085 \pm 0.087	0.076 \pm 0.076	0.085 \pm 0.102	0.085 \pm 0.099	0.073 \pm 0.121
16	0.100 \pm 0.083	0.110 \pm 0.100	0.098 \pm 0.121	0.083 \pm 0.078	0.125 \pm 0.105	0.105 \pm 0.107	0.136 \pm 0.156	0.132 \pm 0.112
17	0.075 \pm 0.073	0.095 \pm 0.049	0.077 \pm 0.056	0.085 \pm 0.064	0.070 \pm 0.066	0.081 \pm 0.057	0.093 \pm 0.077	0.062 \pm 0.066
18	0.071 \pm 0.063	0.058 \pm 0.084	0.072 \pm 0.058	0.067 \pm 0.059	0.074 \pm 0.074	0.085 \pm 0.078	0.080 \pm 0.077	0.062 \pm 0.108
19	0.070 \pm 0.070	0.089 \pm 0.093	0.067 \pm 0.052	0.070 \pm 0.059	0.077 \pm 0.072	0.072 \pm 0.074	0.082 \pm 0.105	0.075 \pm 0.071
20	0.076 \pm 0.065	0.084 \pm 0.070	0.083 \pm 0.094	0.087 \pm 0.066	0.076 \pm 0.104	0.083 \pm 0.078	0.067 \pm 0.069	0.076 \pm 0.067

Chapter 4

Discussion

With a normal human upper limb, we co-ordinate its multiple DOFs to do a task [12]. Our muscles work as a motor to control fine and coarse movements in hand. Our brain always has an idea that of how our hand is positioned in its reachable space. We also have an understanding that how much and which muscles we should flex to do a hand movement [34]. We have leaned to do these different movements over a course of time when we were growing up in form of different activities like using a spoon to eat something or using a key to open a lock. Our brains have understood the mapping and kinematics of our arm and hand movements [35]. It knows how much we should flex our muscles to achieve a motion or a pose. When someone gets an upper limb amputation, they loose a big part of their neuromuscular system (for example: transradial amputation). When a myoelectric prosthesis is attached to the amputated limb, it takes the EMG data from those remnant muscles in the hand, where the electrodes of the prosthesis sit[1][36]. By doing this, it allows these muscles to control the functionality of the prosthesis, thus, filling the gap of the missing limb. But now the users have to learn a new mapping in their brain of using the prosthesis with these new muscles where the electrodes are placed [3].

Therefore, a coding is solved between EMG features and different hand movements with PR techniques to establish an initial relationship between them. This allows controlling the prosthesis. With learning users get better in controlling the prosthesis, they generate high quality EMG patterns[1][10][3][11]. It means that the features that control/define activities become less variable, separable from other features and consistent with demand of the same feature. But we are interested in knowing the reasoning behind this change. Understanding the reasoning and the factors involved can help us make the experience of learning very modular. Users can get a common training in initial training sessions and later their experiences can be personalized based on the outcome of initial training sessions. This way users can be able to exploit the full functionality of their prosthesis and therefore, the

prosthesis rejection rate can decrease.

Henceforth, In this study, we have looked into the activations of different hand movements over multiple user training sessions, and are interested in knowing the underlying mechanisms that cause the increment in performance post-training. We used the concept of muscle synergies and activation coefficients to understand if any of these factors of muscle activation data are the reasoning behind the change in performance, and does these factors change with user training that cause the increase in performance.

For that, we used NMF to calculate the subspaces of muscle activation data, called muscle synergies and muscle activation coefficient patterns [12][18]. During data analysis we faced some problems with our data, but with some participants and some specific matching techniques we were able to look for a variation in the subspaces. Those problems, their reasoning and inferences from the outcomes are discussed in the following paragraphs.

In fixed muscle synergy approach it requires that a limited number of muscle synergies are systematically exploited when muscles are used differently to perform a set of tasks, as in a typical myoelectric prosthesis [6]. With our EMG data we systematically exploited 1-8 muscle synergies. Generally, a few (3-4) muscle synergies are good enough to explain for more than 80% of VAF of the data. After that the next synergy adds only a small amount of VAF (\approx 2-3%). The drastic decrement decides the number of muscle synergies that should be used [20]. But for our data the cumulative difference in VAF was much higher for each dimension (table 3.1), so that optimum number of muscle synergies could not get defined. Instead we chose the dimensionality to be 4 based on an 80% cutoff for VAF, which is not a strong metric to define dimensionality. If a larger number of muscles were recorded instead of only 8, the problem of high cumulative difference would not have been there, because in that scenario, more number of synergies can get extracted, and that will decrease the cumulative VAF. Big cumulative difference can also be a reason for unstable solutions, because there is a big quantity of data which should have been included in the muscle synergy structure was not used.

Later, while working with finding stable solutions, we defined our hypothesis of choosing any solution as a global solution. Following the hypothesis, a solution that have appeared at least twice in any of W10, W25, W50, and W50b is a global solution. But there is a possibility that our hypothesis is wrong and we have worked with local solutions. We also found out that the solutions were sensitive to the initial conditions, therefore, change in initial W and H matrices might have led to a different solution. This can be a reason of mismatch, because we might have tracked the change in synergy structure with wrong solutions. But getting local solutions also indicates that the data is like this. Generally, when solving a *convex* optimization

problem like this, global solutions are achieved [18]. This was verified with simulated data too. For both 8 and 22-muscle data, stable solutions with a correlation coefficient 1 (i.e. exact solutions) were achieved, when compared respectively.

While tracking the change with NDP and CPA we also noticed that synergy mismatches have happened in order of 3 training sessions. It can be noticed easily in figure 3.3 for synergy W2. Also, there were 3 training sessions each day. There can be a possibility that the electrode and muscle combinations got changed when recording the EMG data in a training sessions on a different day. Therefore, our muscle data is altered and hence, in muscle synergy subspace activation jumping to other electrode can be noticed in order of 3 training sessions.

Though even after these possibilities, a change in muscle synergy and activation coefficient structure was tracked successfully with k-means clustering for P3 and P19, which is represented in figures 3.6, 3.7, 3.8, and 3.9. Yet, when looked only for average initial and average final behaviour, a change in muscle synergy and activation coefficient structure was achieved correctly for 14 participants (except for P6, P7, P8, P17, P18, and P19). Therefore, with user training, muscle synergy and activation coefficient structure changes. Even though, if a day-wise mismatch of electrodes had happened, a change was noticed in terms of NDP and CPA over the same day training sessions too.

When working with k-means clustering, we pooled all the synergies for each participant and clustered them into four groups to match them. Four numbers of clusters were chosen because the dimensionality of the solutions is four. But, when we calculated optimal numbers of clusters with ‘Calinski-Harabasz Criterion’ for each participant [37], they were varying in the range of 5-7 for different participants. It means that 5-7 numbers of independent synergies can exist. If we have had extracted optimal numbers of clusters for each participant (i.e dimensionality = optimal clusters), there could have been the following possibilities. Firstly, the NMF could have given approximate solutions as well as we could have got better matches of solutions with NDP or CPA. This could have led to better tracking and lesser mismatches. Secondly, our clustering by k-means could have given better results which could have given some logical pattern recognition with the available data.

Although, a change was seen in the sub-spaces over training sessions for a few participants, a successful case would have happened if for all participants the data would have been able to give an approximate solution to the global minima of error. Also, the decision of dimensionality should have been based on selection of optimum number of basis vectors. Because of all these problems it is safe to say that the data was not good enough to apply NMF on it. Tracking the change in structure of sub-spaces would have been much easier if we were recording EMG data from more (≈ 20) muscles. A few of them should have been used to generate the control

commands like a typical prosthesis, and rest of them could be used for feedback and tracking the synergy structure. This is what we had planned initially.

Chapter 5

Conclusion

Muscle synergy and activation coefficient patterns both change over learning to use a PR based prosthesis. New fixed muscle synergies build up after every training session. With changing muscle synergies, activation coefficients also change. This was systematically demonstrated for P3 and P19. Tracking for them was achieved successfully from training session-1 to training session-15. When only looked for initial and final averaged behavior, the change was acquired correctly for 14 participants. The average change in muscle synergies is defined numerically in terms of CPA that gives an angular measure of change in a two dimensional vector space. Muscle activation coefficient patterns are defined as $\text{mean} \pm \text{SD}$ for each pattern. This gives the idea of mean variation and a spread of activations from mean that exist to execute a task. A change in mean value indicates if most of the activations are changing towards the new mean, and a change in SD means that separability of different activities within the same pattern is changing.

As a future work, it should be preferred to do the whole experiment again with a larger number of electrodes. That way it will be easier and systematic to track the change with NDP and CPA. Having extra information will never be an issue, because then we can be selective, as well as, can choose to work with only those muscles we are interested in. While clustering the synergies it was noticed that optimum number of clusters can be more than the dimensionality of the solutions. It means that if a synergy is exploiting one structure in first training session, it can get totally changed to something else, which is not similar to any other muscle synergy structures of the first training session. Therefore, synergies should be categorized more freely into optimum number of clusters. If a synergy of first training session jumps to another new cluster in second or subsequent training sessions, it will showcase that the structure of that synergy has got changed. This is also a way to visualize the change which was not exploited in this study and can be done as a future work.

Ethics

Assistive technology devices use neural signals from brain or muscles for human-machine interfacing to access the information that brain sends to different muscles for their control. We accessed this information from able bodied participants' non-dominant hand with a myoelectric-controlled interface. In that, 8-electrodes were pasted equidistantly around the thickest part of the non-dominant hand with help of a brace. We did peripheral measurements of activations from muscles with a training exercise, where participants need to perform eight hand movements: rest, wrist supination, wrist pronation, wrist flexion, wrist extension, hand open, fine pinch grip, and lateral thumb grip. EMG data for each training session which consisted these hand movements were stored for further calculations. In these experiments, though our participants were human subjects, but any kind of invasive measurements were not performed. Measurements were also performed with peripheral nervous system, that only allows to read the neural signal and does not allow to alter it in any way. This is a standard procedure for EMG measurements [38] [39].

Participants were also informed about the whole procedure of recordings and were asked to sign a letter of consent too. All data processing techniques were standard, and were followed from published sources. This study holds an added value for the society too. Understanding learning to control a prosthesis and related changes in muscle activations can help amputated people learn to control their prosthesis in a robust way in a comparatively short time.

This study was approved by the ethical committee of the Department of Human Movement Sciences at the University Medical Center Groningen (UMCG).
(ECB/2017.01.121)

Appendix

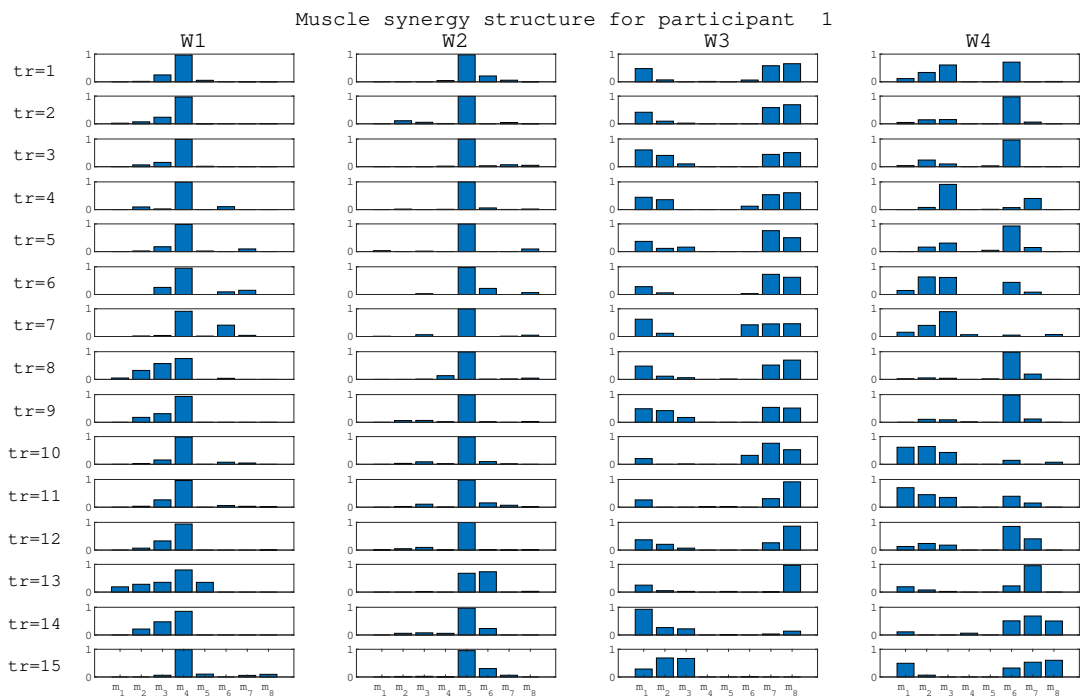


Figure 5.1: Bar-graphs of four muscle synergies (W1-W4) over training sessions (tr) for participant 1, matching is done by NDP (or CPA), m_1 to m_8 on x-axis represent 8-muscles, bars show the fixed muscle synergy activations of muscles

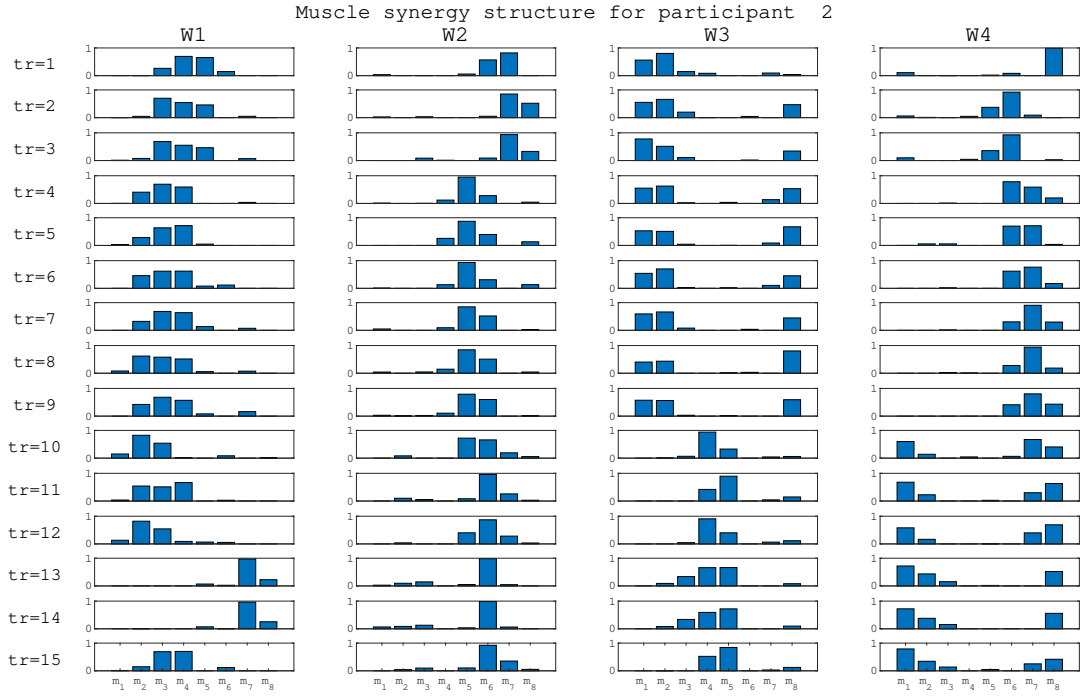


Figure 5.2: Bar-graphs of four muscle synergies (W1-W4) over training sessions (tr) for participant 2, matching is done by NDP (or CPA), m_1 to m_8 on x-axis represent 8-muscles, bars show the fixed muscle synergy activations of muscles

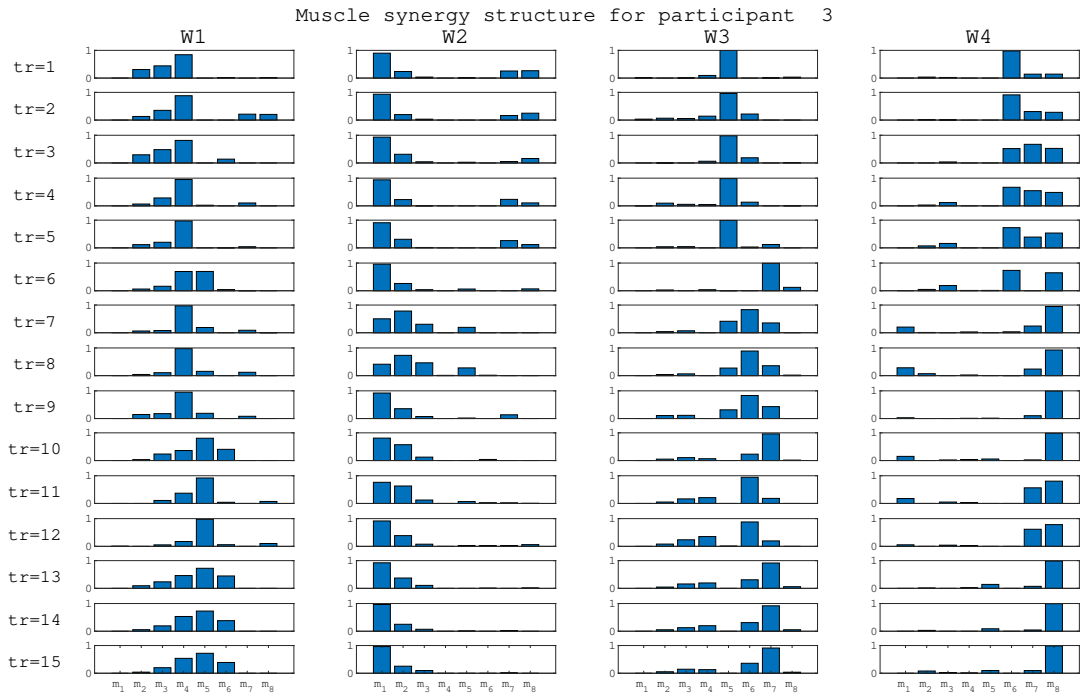


Figure 5.3: Bar-graphs of four muscle synergies (W1-W4) over training sessions (tr) for participant 3, matching is done by NDP (or CPA), m_1 to m_8 on x-axis represent 8-muscles, bars show the fixed muscle synergy activations of muscles

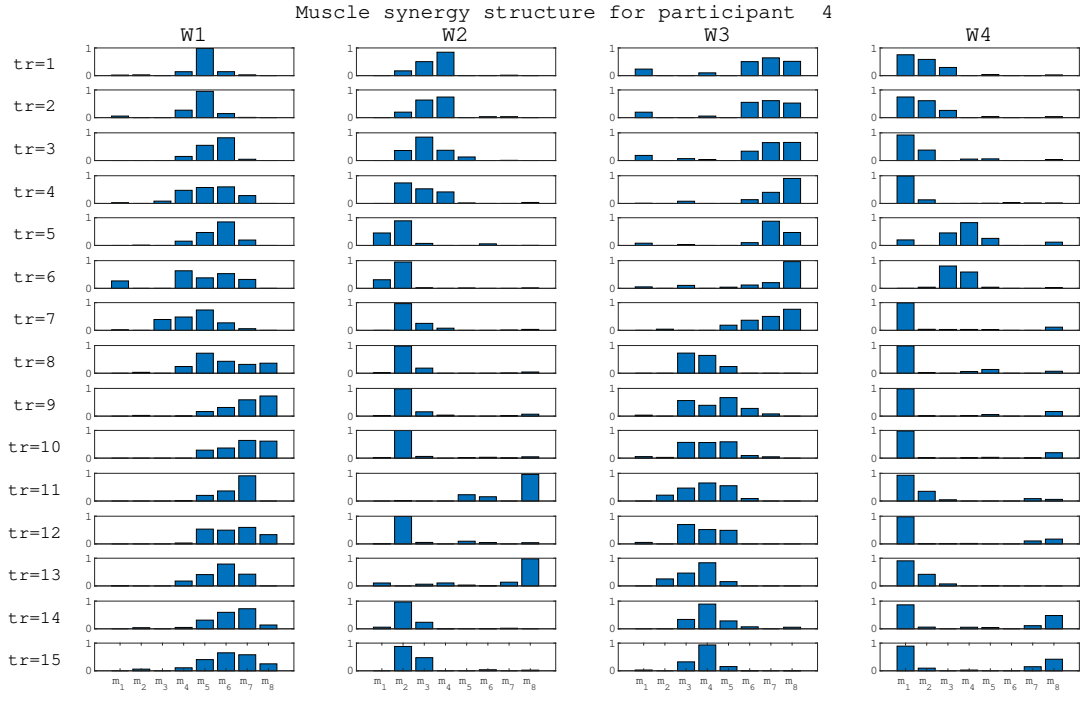


Figure 5.4: Bar-graphs of four muscle synergies (W1-W4) over training sessions (tr) for participant 4, matching is done by NDP (or CPA), m_1 to m_8 on x-axis represent 8-muscles, bars show the fixed muscle synergy activations of muscles

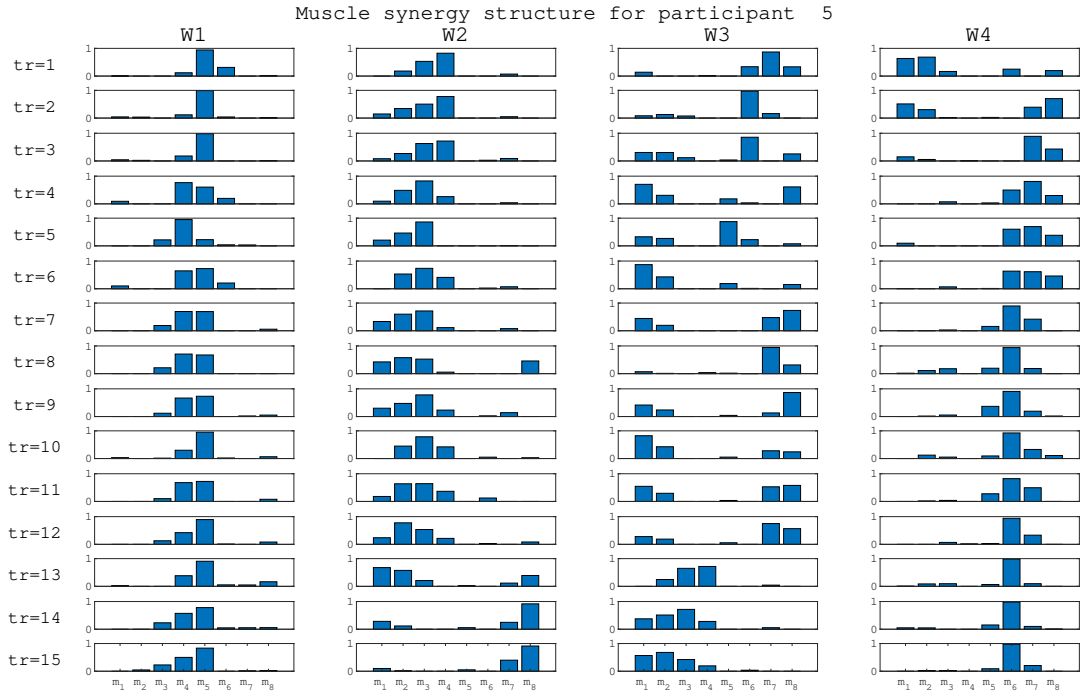


Figure 5.5: Bar-graphs of four muscle synergies (W1-W4) over training sessions (tr) for participant 5, matching is done by NDP (or CPA), m_1 to m_8 on x-axis represent 8-muscles, bars show the fixed muscle synergy activations of muscles

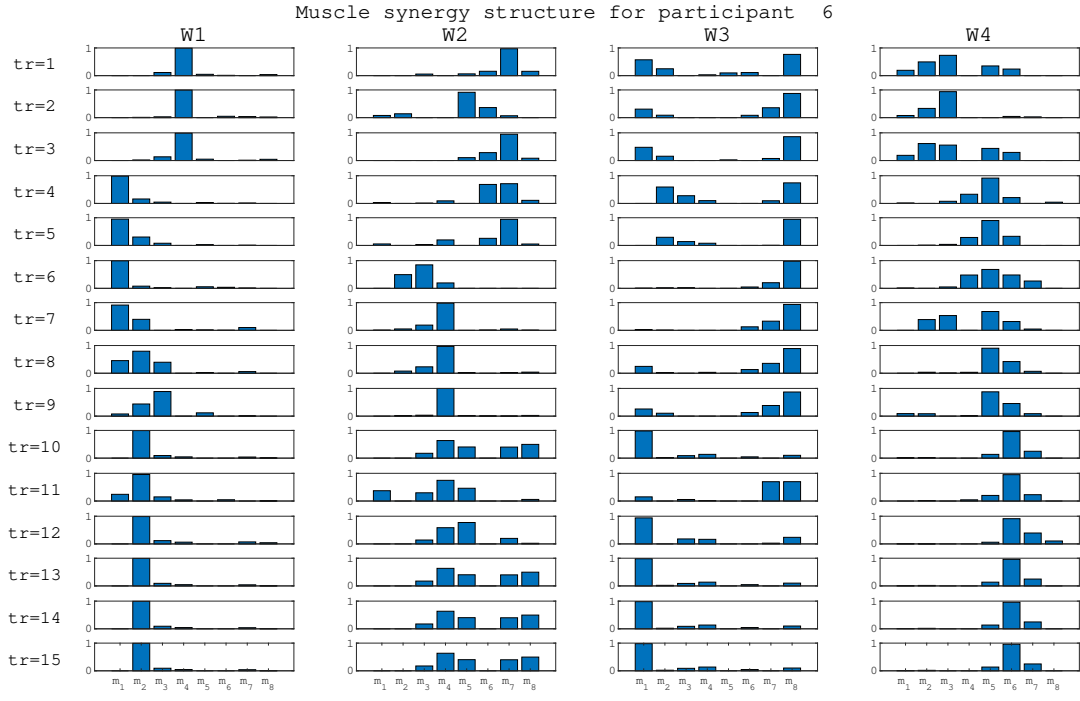


Figure 5.6: Bar-graphs of four muscle synergies (W1-W4) over training sessions (tr) for participant 6, matching is done by NDP (or CPA), m_1 to m_8 on x-axis represent 8-muscles, bars show the fixed muscle synergy activations of muscles

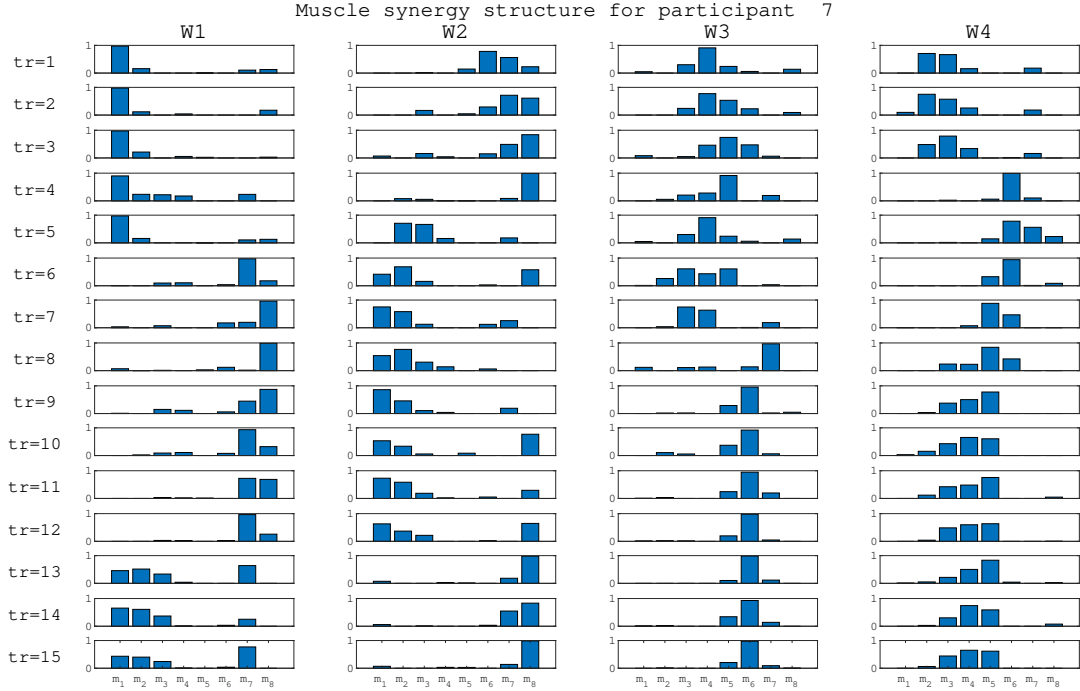


Figure 5.7: Bar-graphs of four muscle synergies (W1-W4) over training sessions (tr) for participant 7, matching is done by NDP (or CPA), m_1 to m_8 on x-axis represent 8-muscles, bars show the fixed muscle synergy activations of muscles

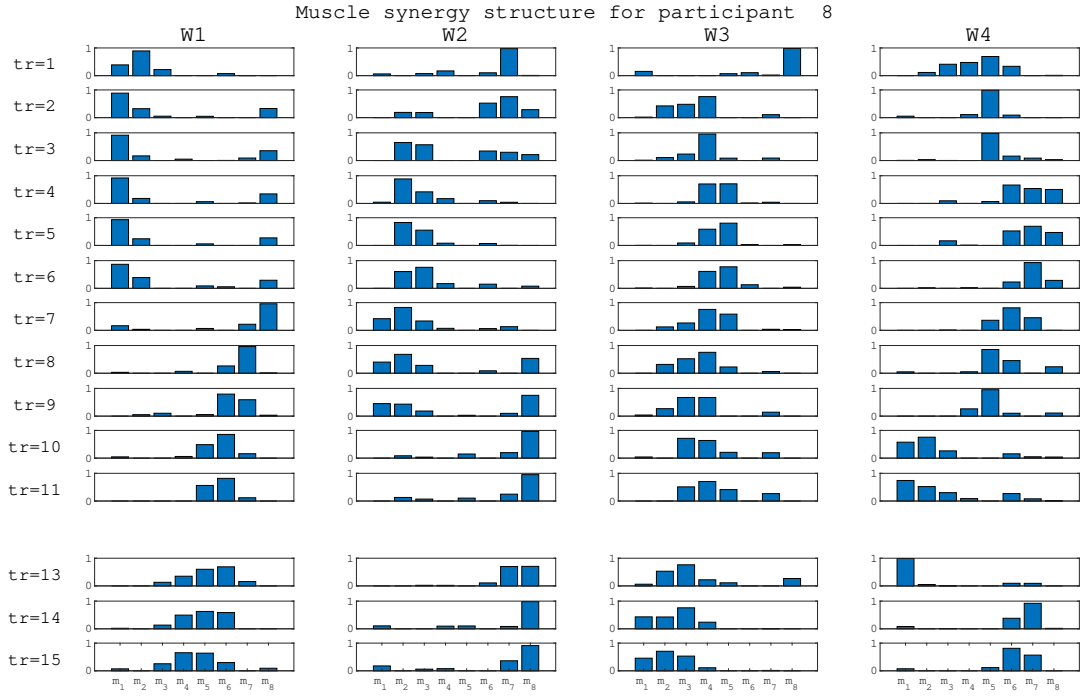


Figure 5.8: Bar-graphs of four muscle synergies (W1-W4) over training sessions (tr) for participant 8, matching is done by NDP (or CPA), m_1 to m_8 on x-axis represent 8-muscles, bars show the fixed muscle synergy activations of muscles

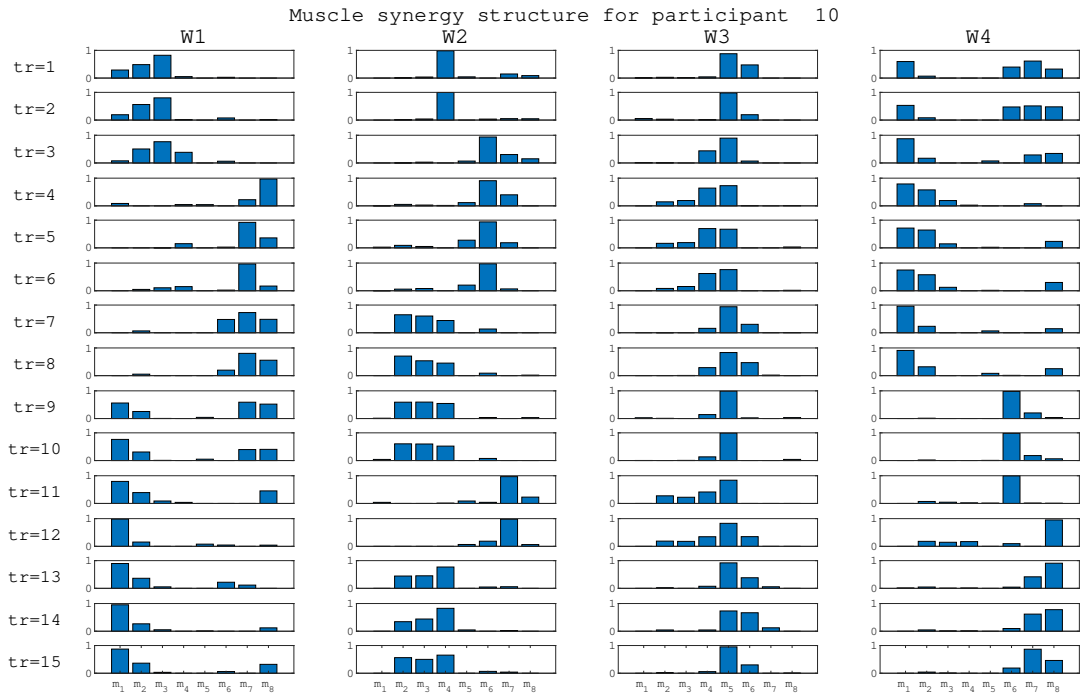


Figure 5.9: Bar-graphs of four muscle synergies (W1-W4) over training sessions (tr) for participant 10, matching is done by NDP (or CPA), m_1 to m_8 on x-axis represent 8-muscles, bars show the fixed muscle synergy activations of muscles

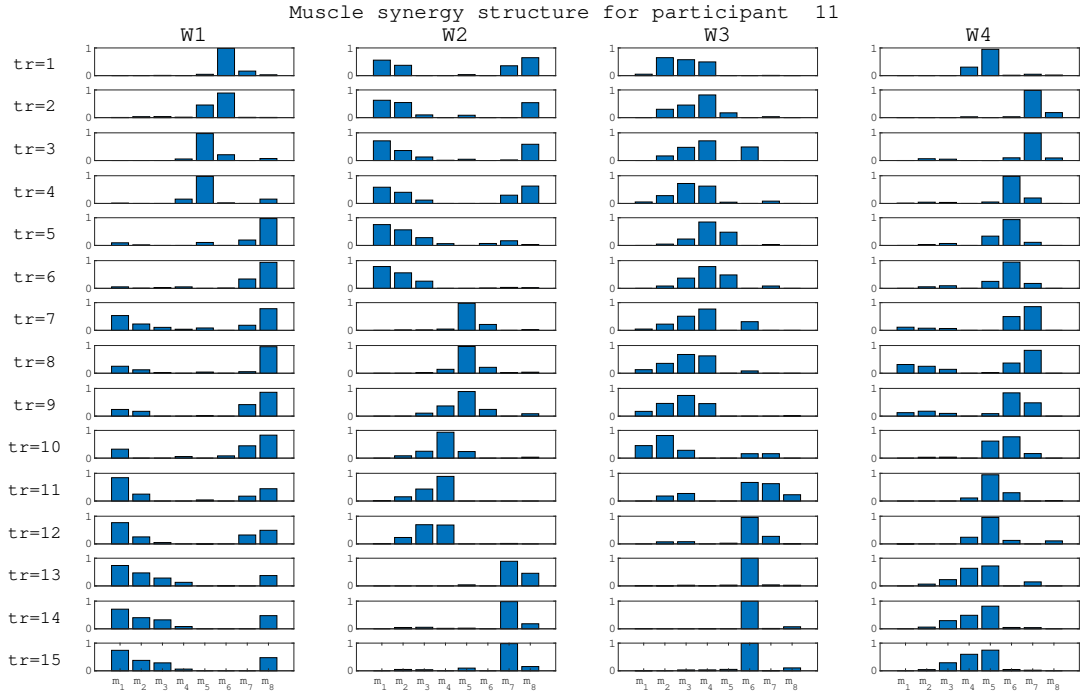


Figure 5.10: Bar-graphs of four muscle synergies (W1-W4) over training sessions (tr) for participant 11, matching is done by NDP (or CPA), m_1 to m_8 on x-axis represent 8-muscles, bars show the fixed muscle synergy activations of muscles

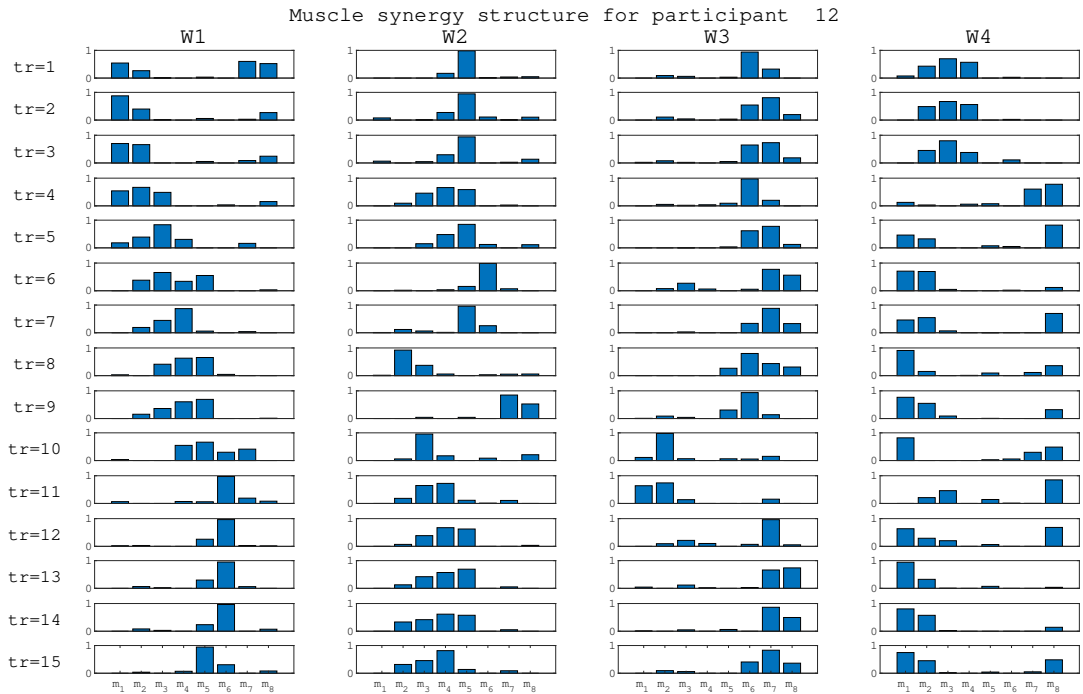


Figure 5.11: Bar-graphs of four muscle synergies (W1-W4) over training sessions (tr) for participant 12, matching is done by NDP (or CPA), m_1 to m_8 on x-axis represent 8-muscles, bars show the fixed muscle synergy activations of muscles

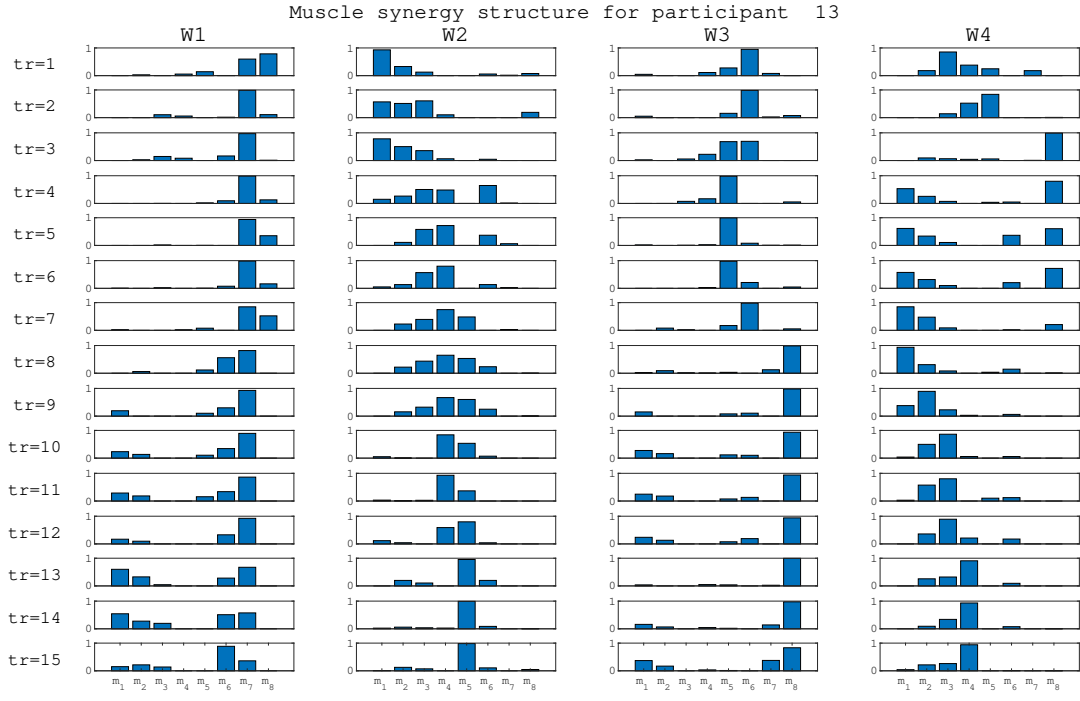


Figure 5.12: Bar-graphs of four muscle synergies (W1-W4) over training sessions (tr) for participant 13, matching is done by NDP (or CPA), m_1 to m_8 on x-axis represent 8-muscles, bars show the fixed muscle synergy activations of muscles

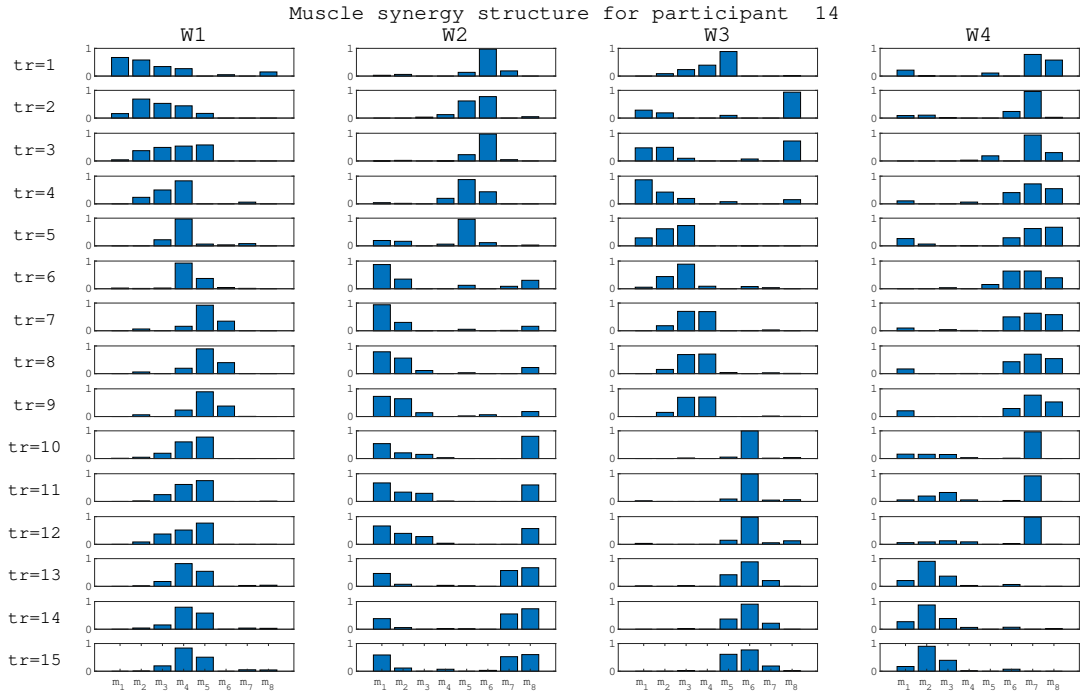


Figure 5.13: Bar-graphs of four muscle synergies (W1-W4) over training sessions (tr) for participant 14, matching is done by NDP (or CPA), m_1 to m_8 on x-axis represent 8-muscles, bars show the fixed muscle synergy activations of muscles

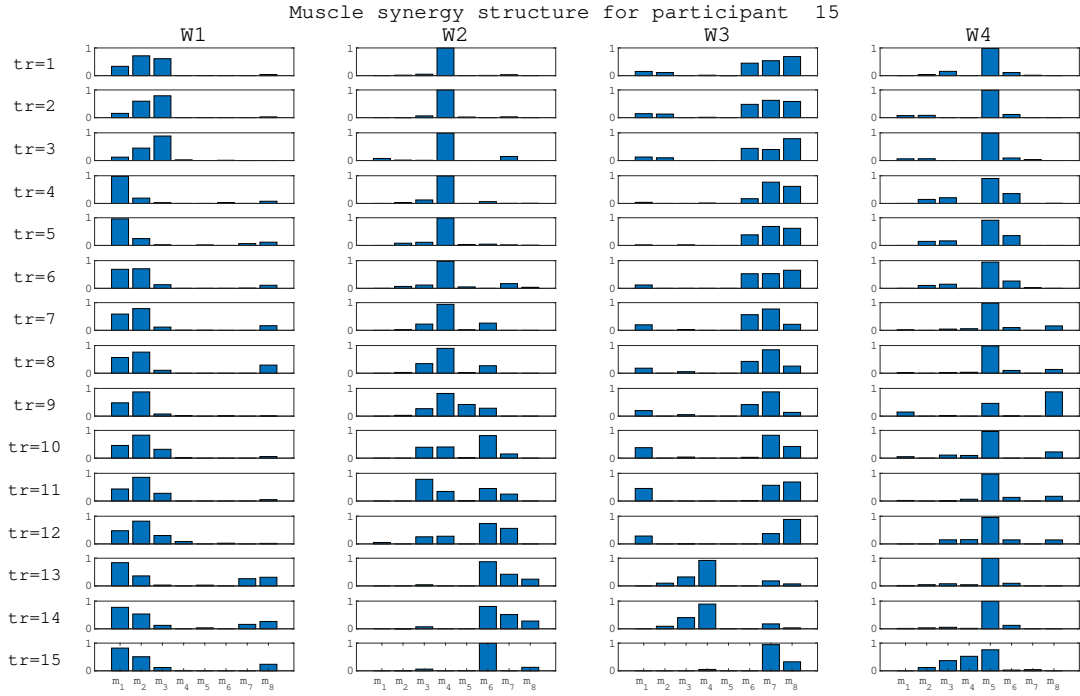


Figure 5.14: Bar-graphs of four muscle synergies (W1-W4) over training sessions (tr) for participant 15, matching is done by NDP (or CPA), m_1 to m_8 on x-axis represent 8-muscles, bars show the fixed muscle synergy activations of muscles

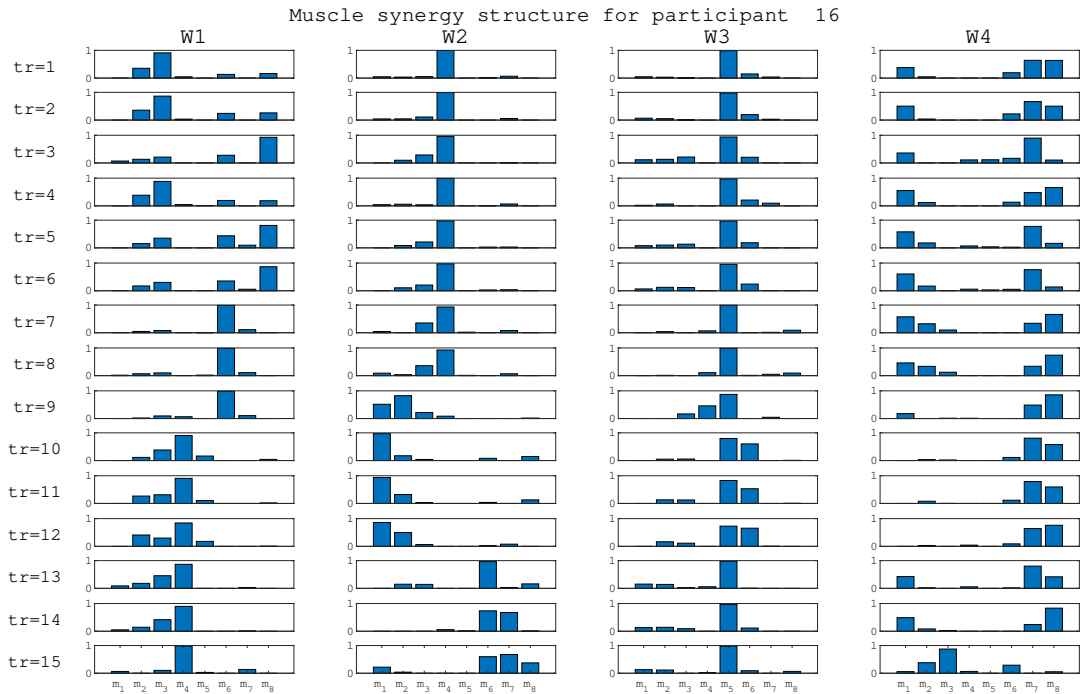


Figure 5.15: Bar-graphs of four muscle synergies (W1-W4) over training sessions (tr) for participant 16, matching is done by NDP (or CPA), m_1 to m_8 on x-axis represent 8-muscles, bars show the fixed muscle synergy activations of muscles

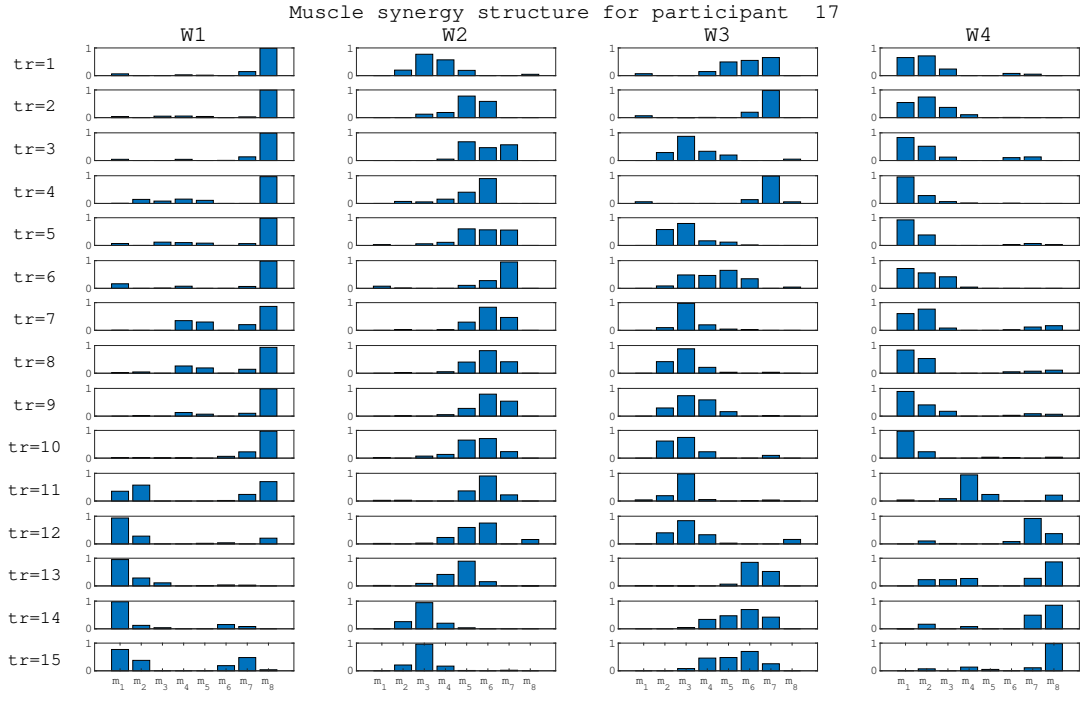


Figure 5.16: Bar-graphs of four muscle synergies (W1-W4) over training sessions (tr) for participant 17, matching is done by NDP (or CPA), m_1 to m_8 on x-axis represent 8-muscles, bars show the fixed muscle synergy activations of muscles

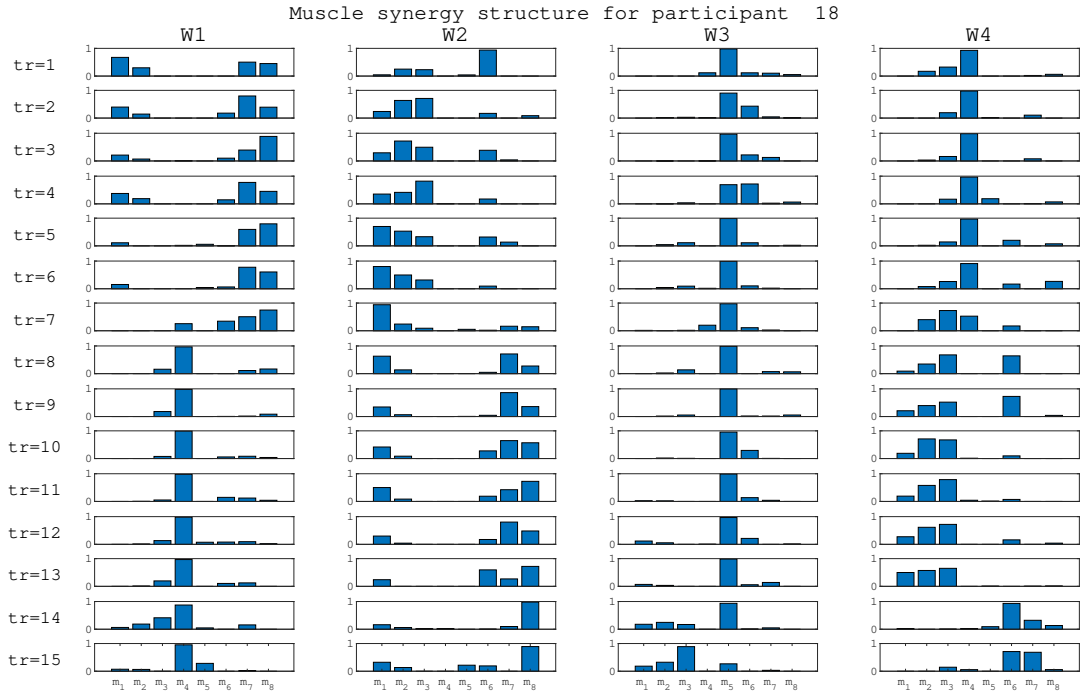


Figure 5.17: Bar-graphs of four muscle synergies (W1-W4) over training sessions (tr) for participant 18, matching is done by NDP (or CPA), m_1 to m_8 on x-axis represent 8-muscles, bars show the fixed muscle synergy activations of muscles

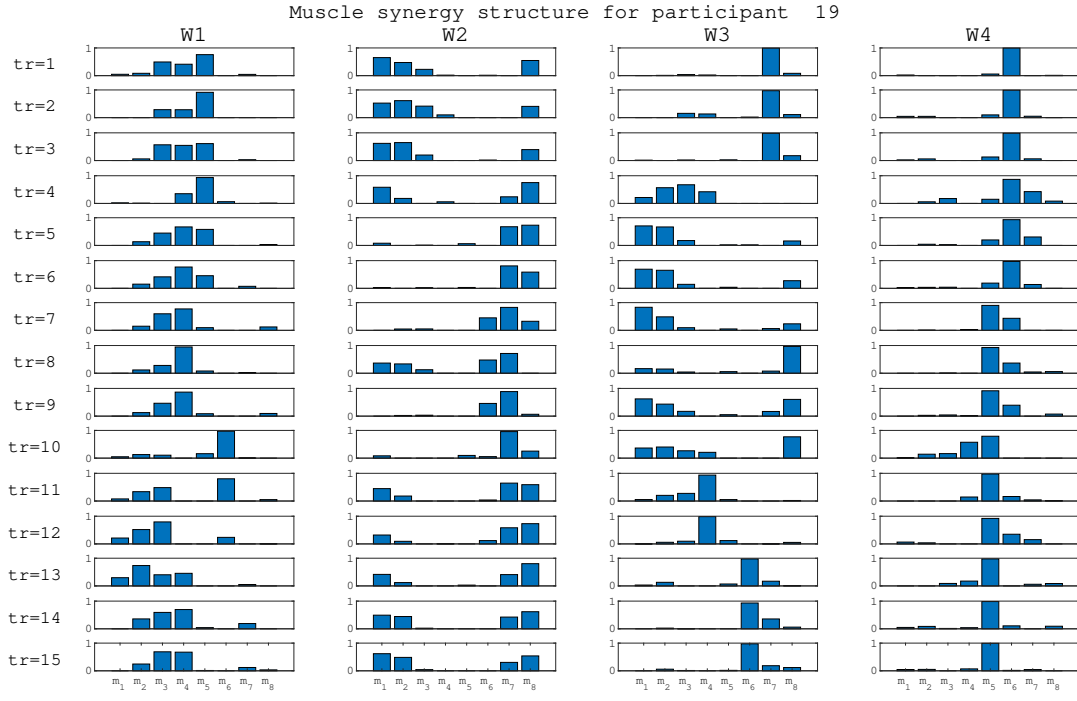


Figure 5.18: Bar-graphs of four muscle synergies (W1-W4) over training sessions (tr) for participant 19, matching is done by NDP (or CPA), m_1 to m_8 on x-axis represent 8-muscles, bars show the fixed muscle synergy activations of muscles

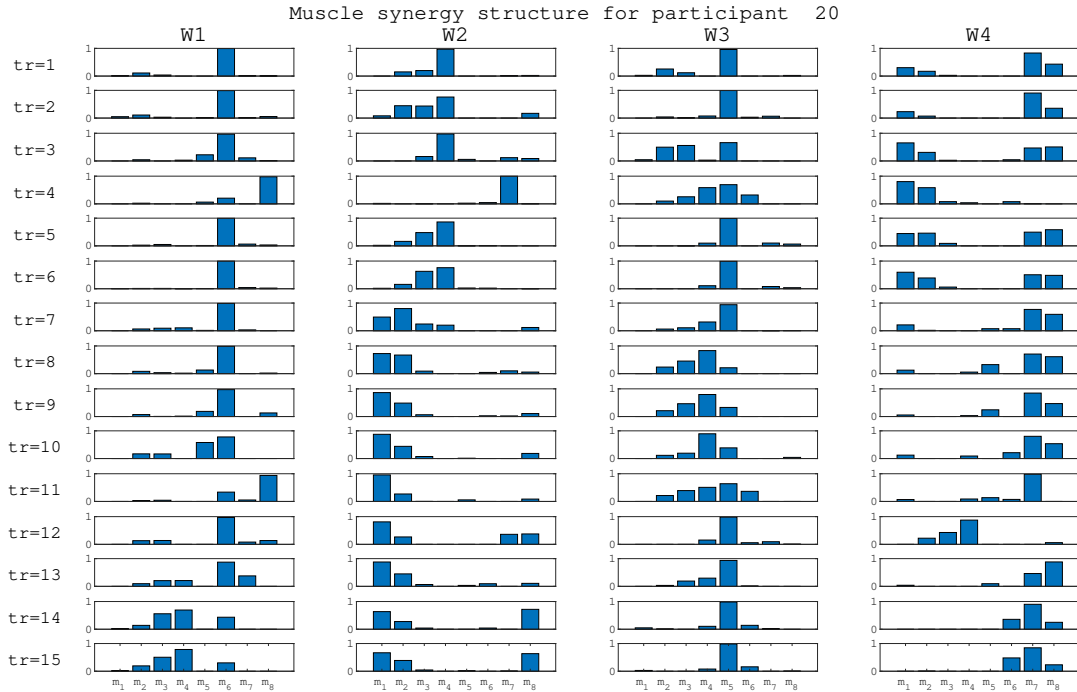


Figure 5.19: Bar-graphs of four muscle synergies (W1-W4) over training sessions (tr) for participant 20, matching is done by NDP (or CPA), m_1 to m_8 on x-axis represent 8-muscles, bars show the fixed muscle synergy activations of muscles

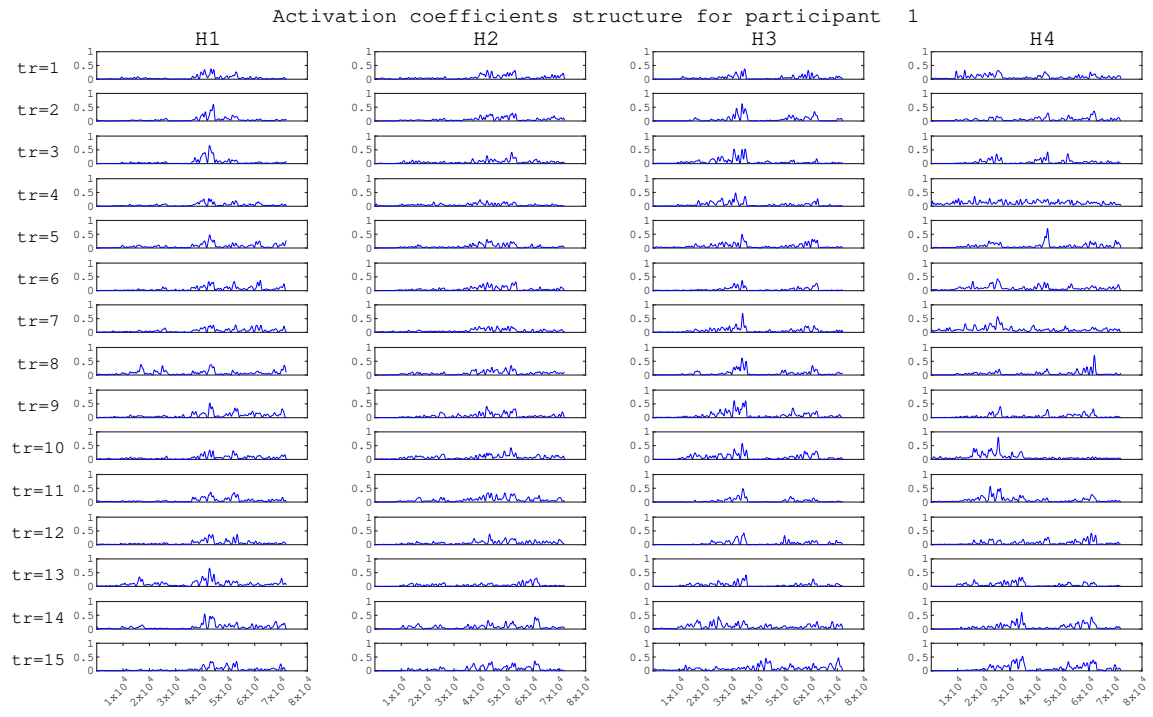


Figure 5.20: Change in four activation coefficient patterns (H1-H4) over training sessions (tr) for participant 1, matching is adopted from the matching of related muscle synergies, X-axis represents number of total observed points

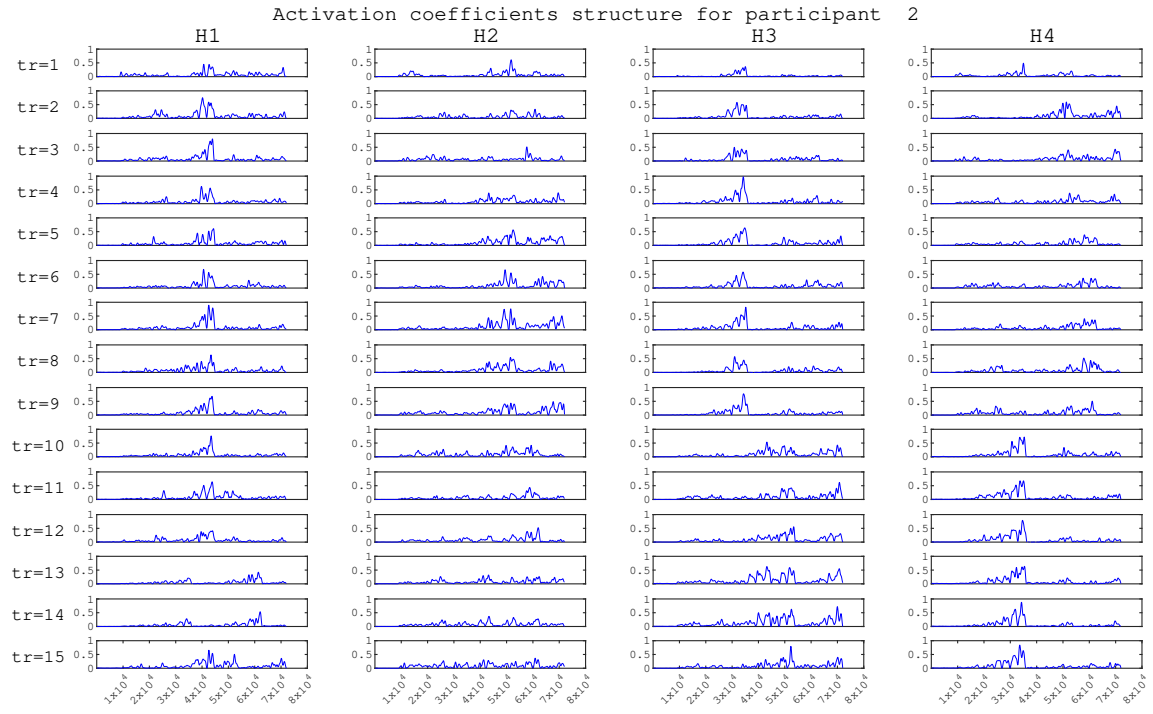


Figure 5.21: Change in four activation coefficient patterns (H1-H4) over training sessions (tr) for participant 2, matching is adopted from the matching of related muscle synergies, X-axis represents number of total observed points

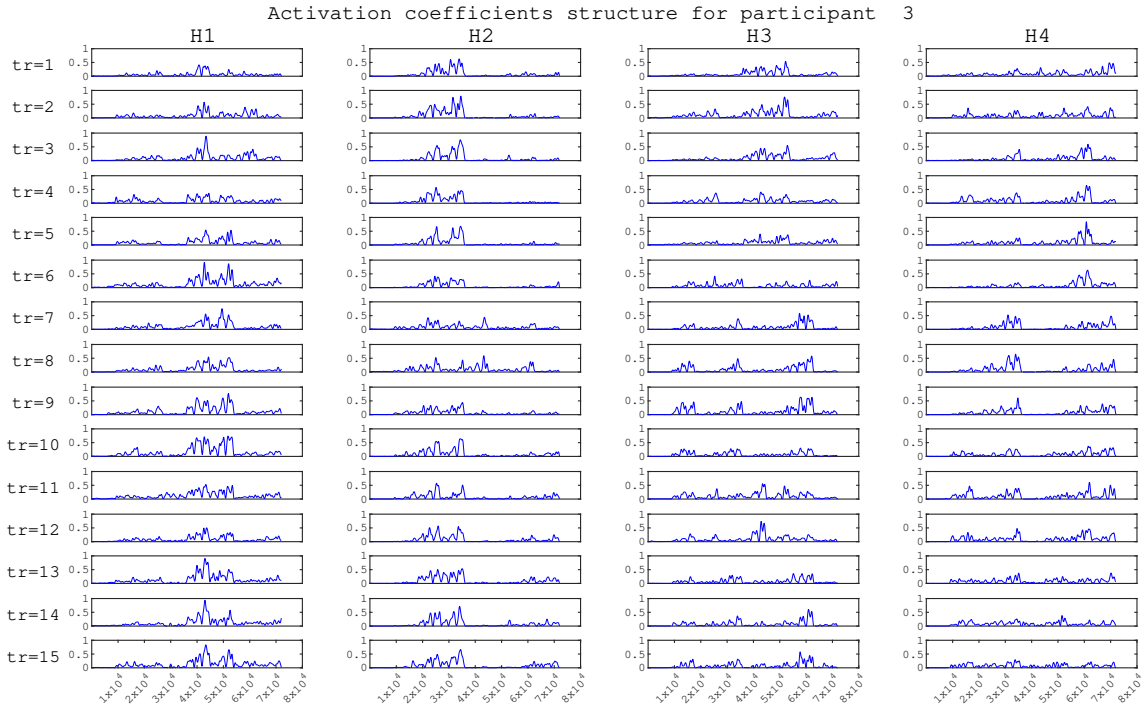


Figure 5.22: Change in four activation coefficient patterns (H1-H4) over training sessions (tr) for participant 3, matching is adopted from the matching of related muscle synergies, X-axis represents number of total observed points

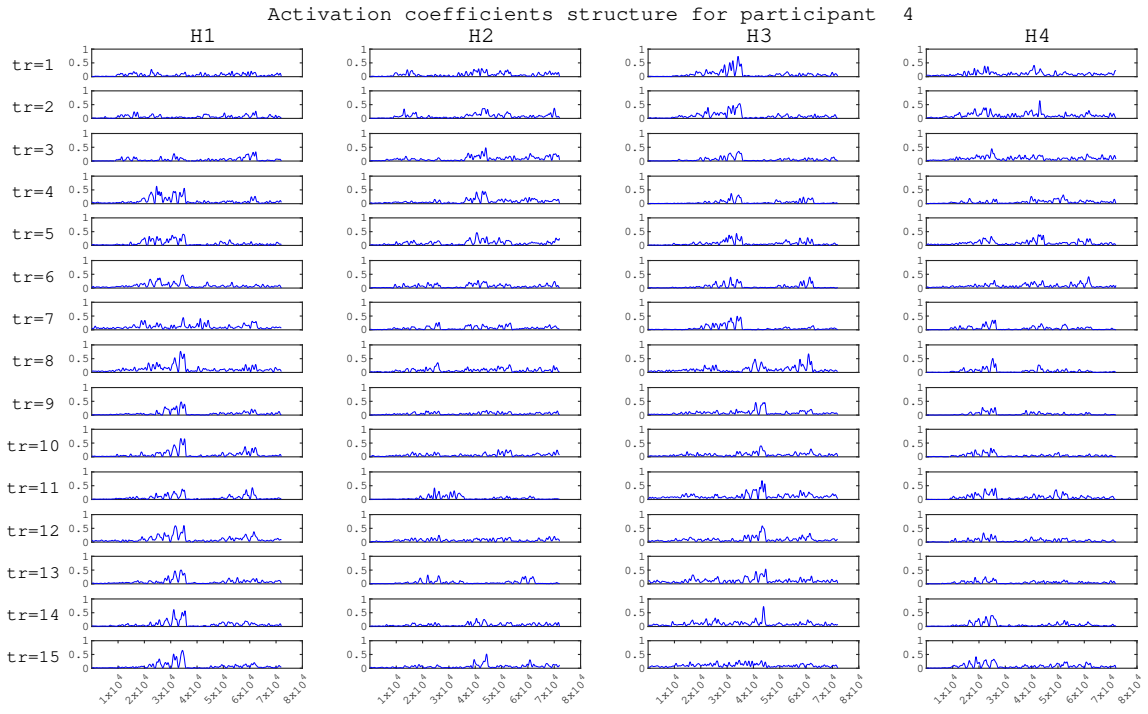


Figure 5.23: Change in four activation coefficient patterns (H1-H4) over training sessions (tr) for participant 4, matching is adopted from the matching of related muscle synergies, X-axis represents number of total observed points

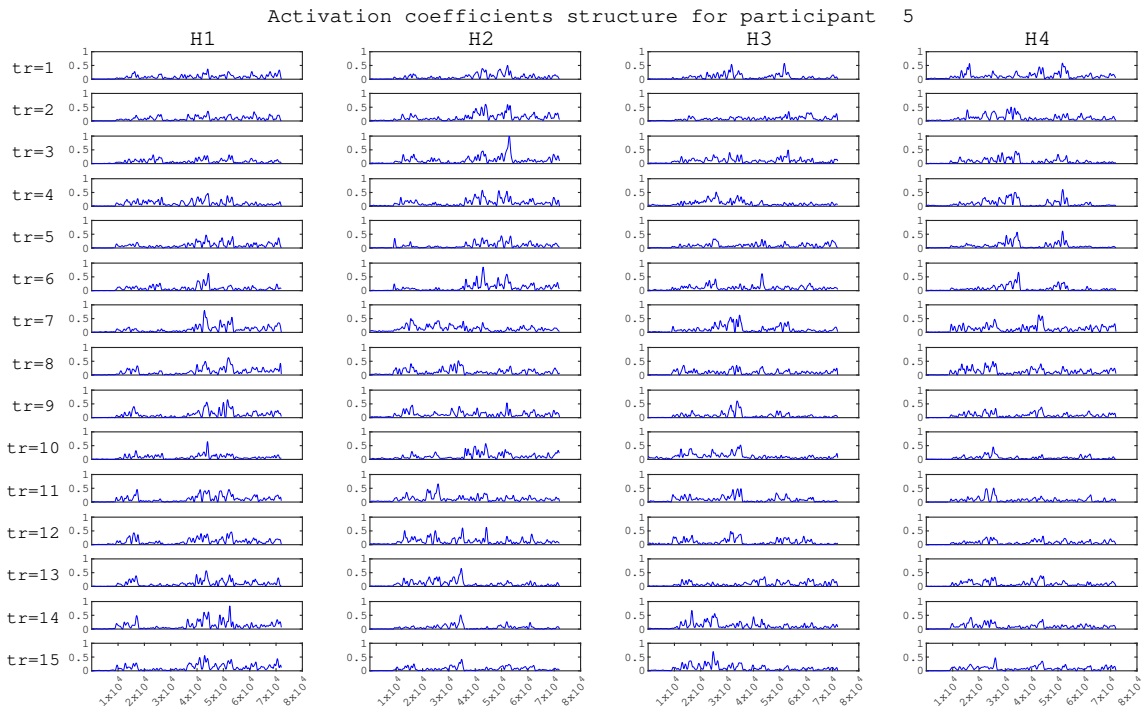


Figure 5.24: Change in four activation coefficient patterns (H1-H4) over training sessions (tr) for participant 5, matching is adopted from the matching of related muscle synergies, X-axis represents number of total observed points

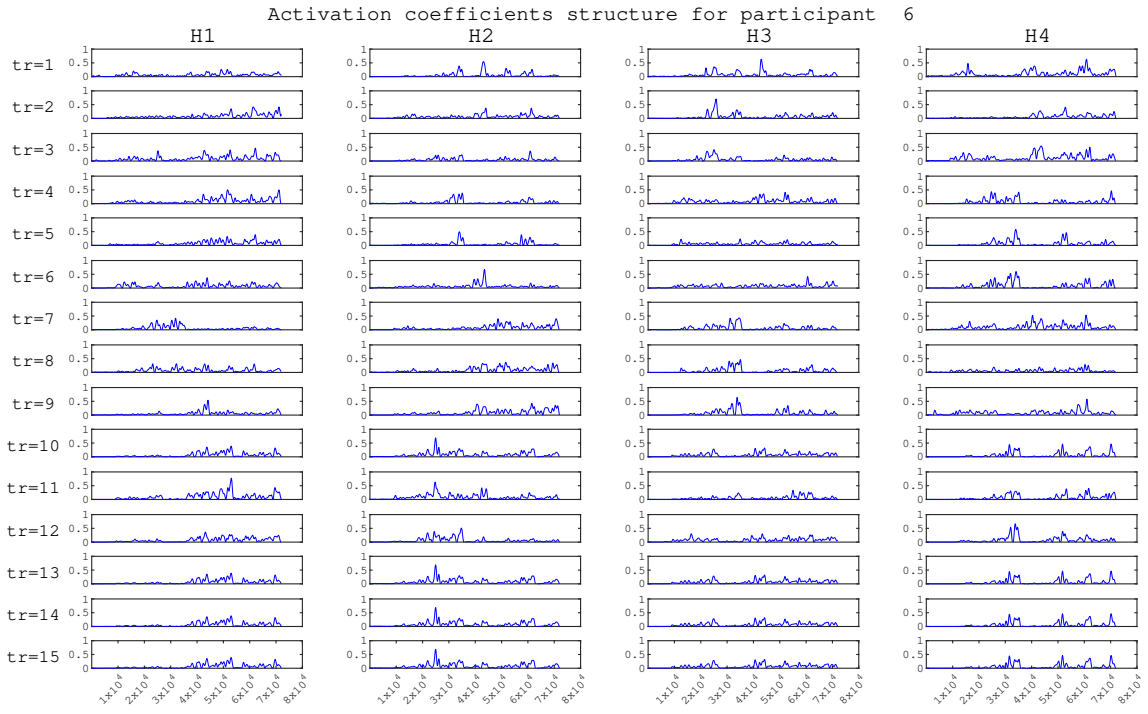


Figure 5.25: Change in four activation coefficient patterns (H1-H4) over training sessions (tr) for participant 6, matching is adopted from the matching of related muscle synergies, X-axis represents number of total observed points

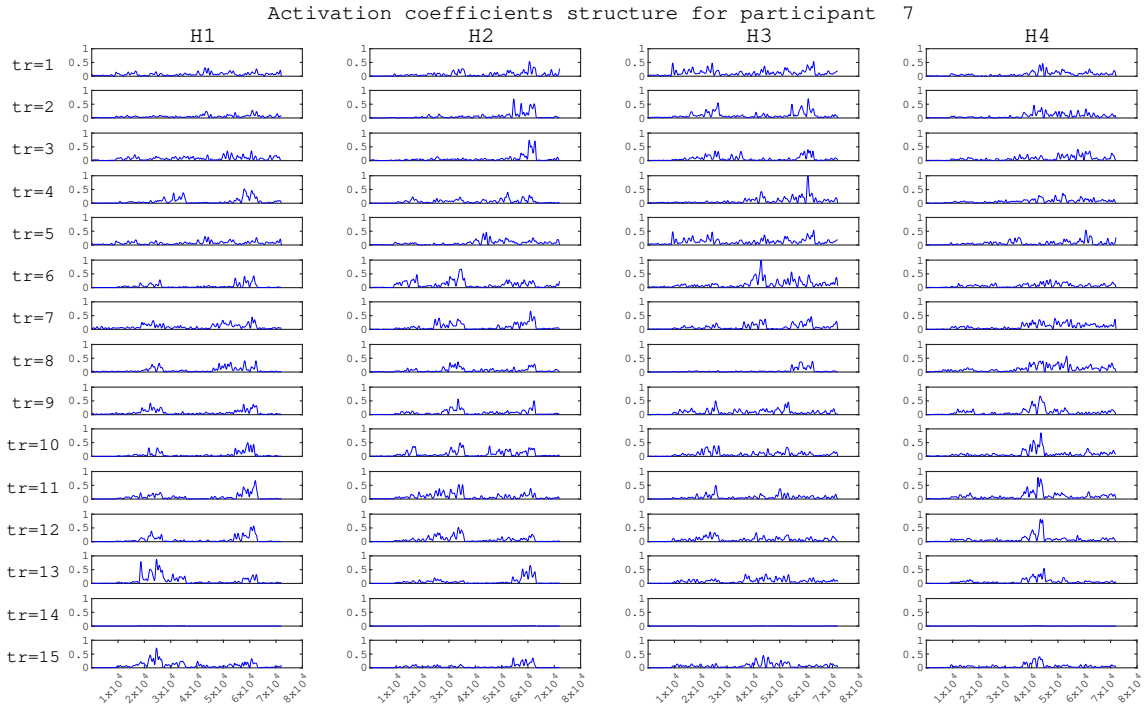


Figure 5.26: Change in four activation coefficient patterns (H1-H4) over training sessions (tr) for participant 7, matching is adopted from the matching of related muscle synergies, X-axis represents number of total observed points

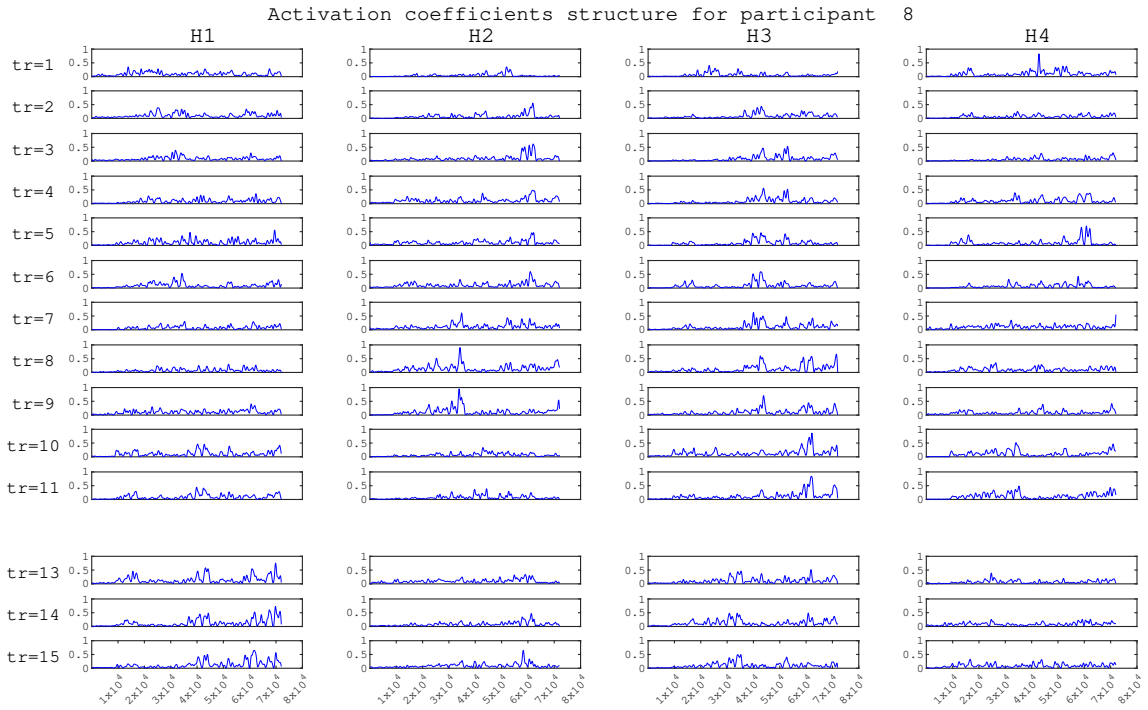


Figure 5.27: Change in four activation coefficient patterns (H1-H4) over training sessions (tr) for participant 8, matching is adopted from the matching of related muscle synergies, X-axis represents number of total observed points

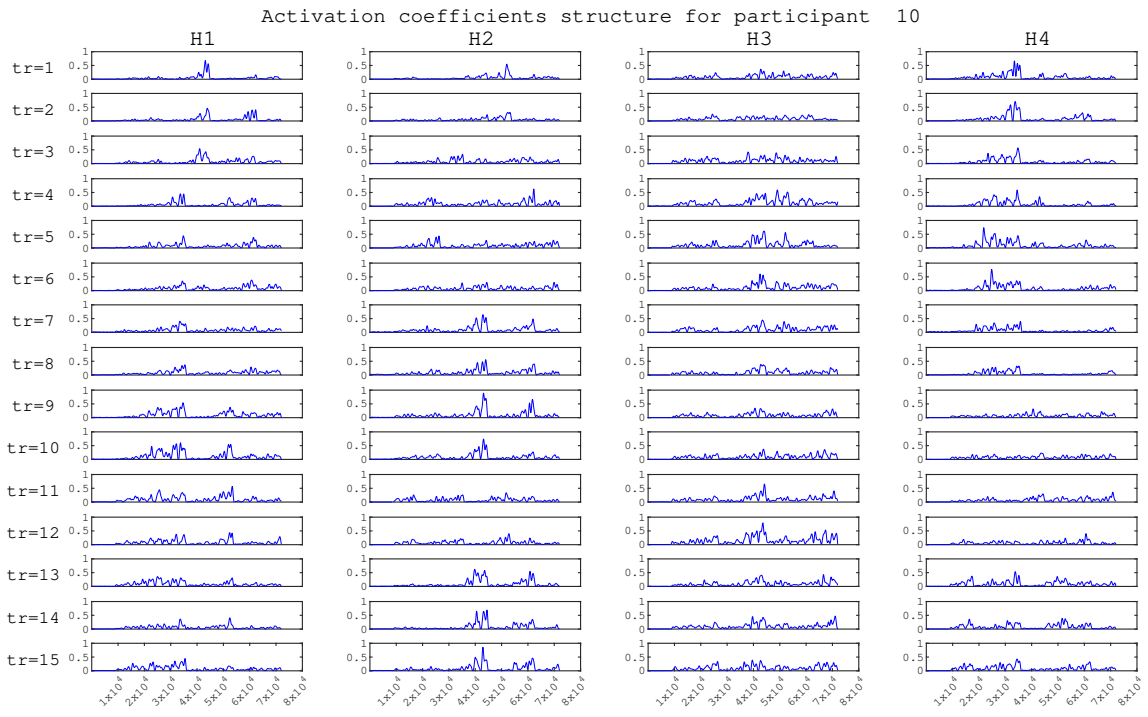


Figure 5.28: Change in four activation coefficient patterns (H1-H4) over training sessions (tr) for participant 10, matching is adopted from the matching of related muscle synergies, X-axis represents number of total observed points

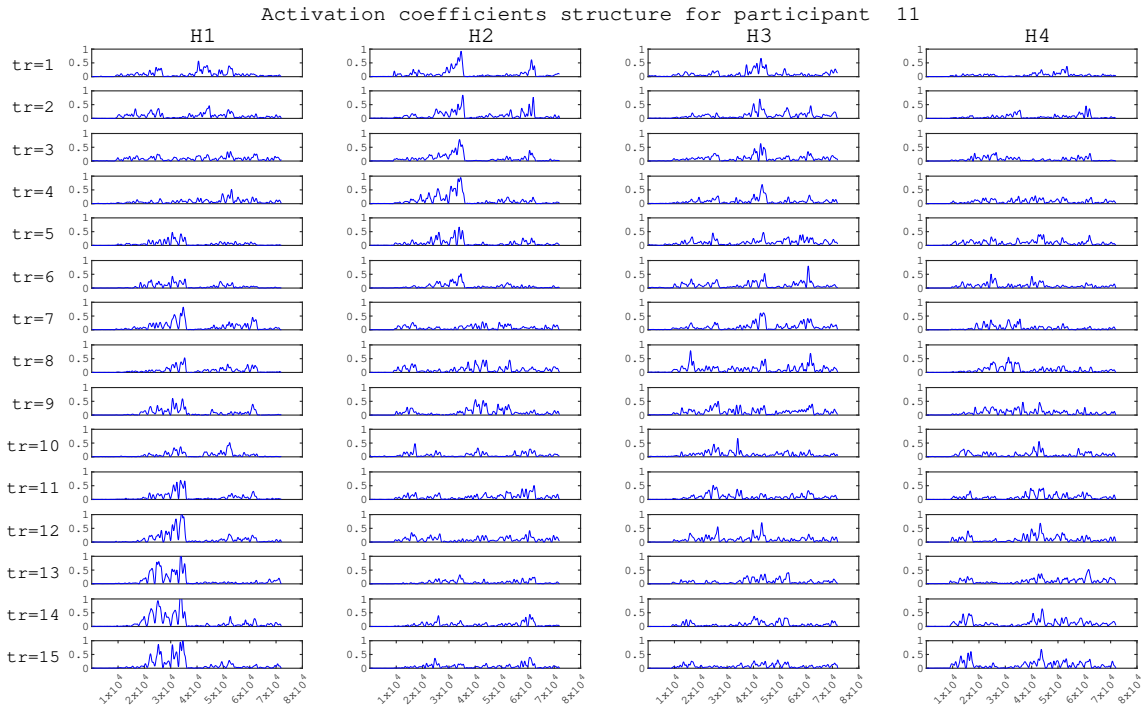


Figure 5.29: Change in four activation coefficient patterns (H1-H4) over training sessions (tr) for participant 11, matching is adopted from the matching of related muscle synergies, X-axis represents number of total observed points

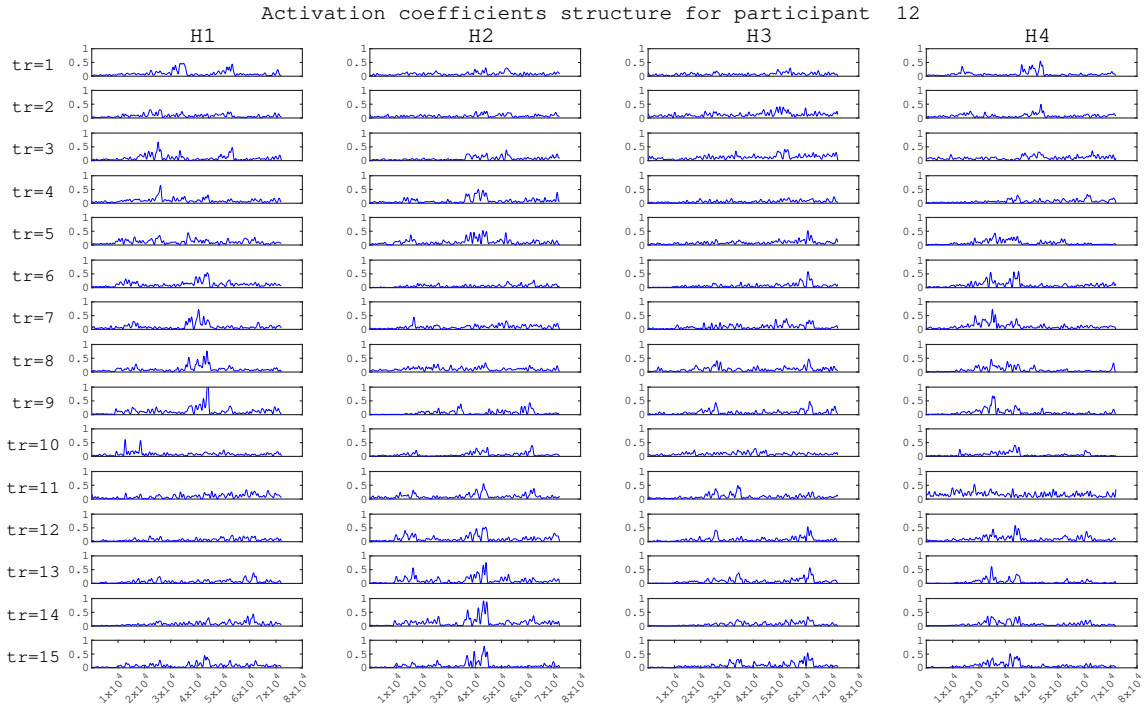


Figure 5.30: Change in four activation coefficient patterns (H1-H4) over training sessions (tr) for participant 12, matching is adopted from the matching of related muscle synergies, X-axis represents number of total observed points

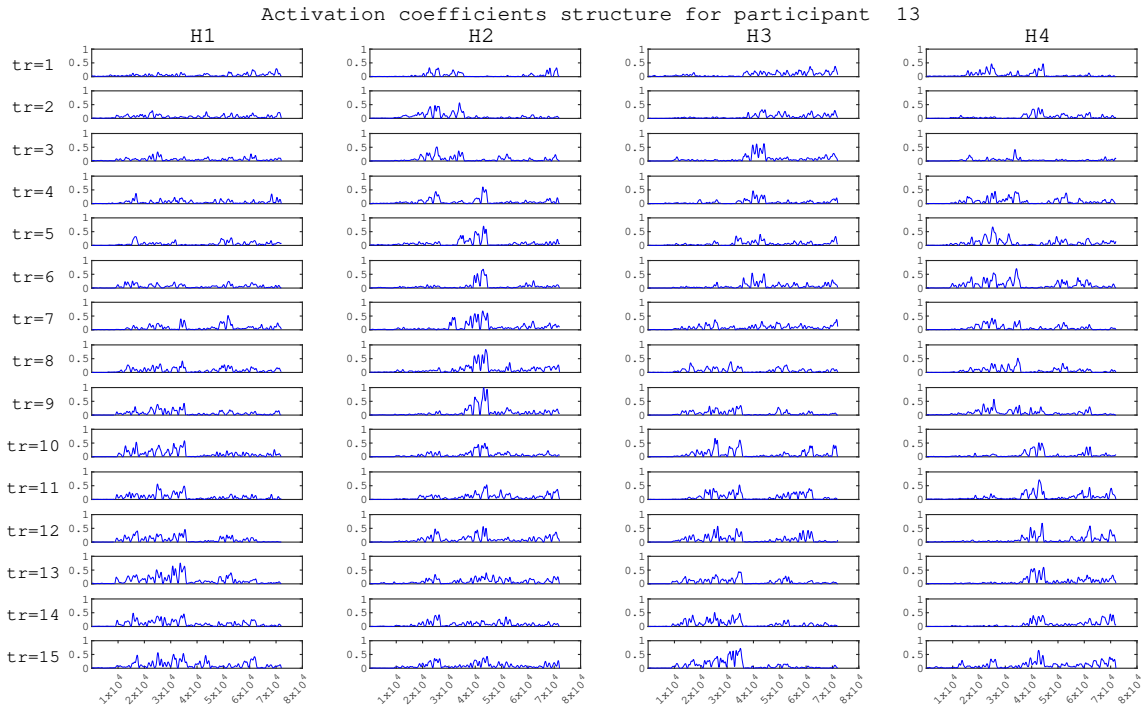


Figure 5.31: Change in four activation coefficient patterns (H1-H4) over training sessions (tr) for participant 13, matching is adopted from the matching of related muscle synergies, X-axis represents number of total observed points

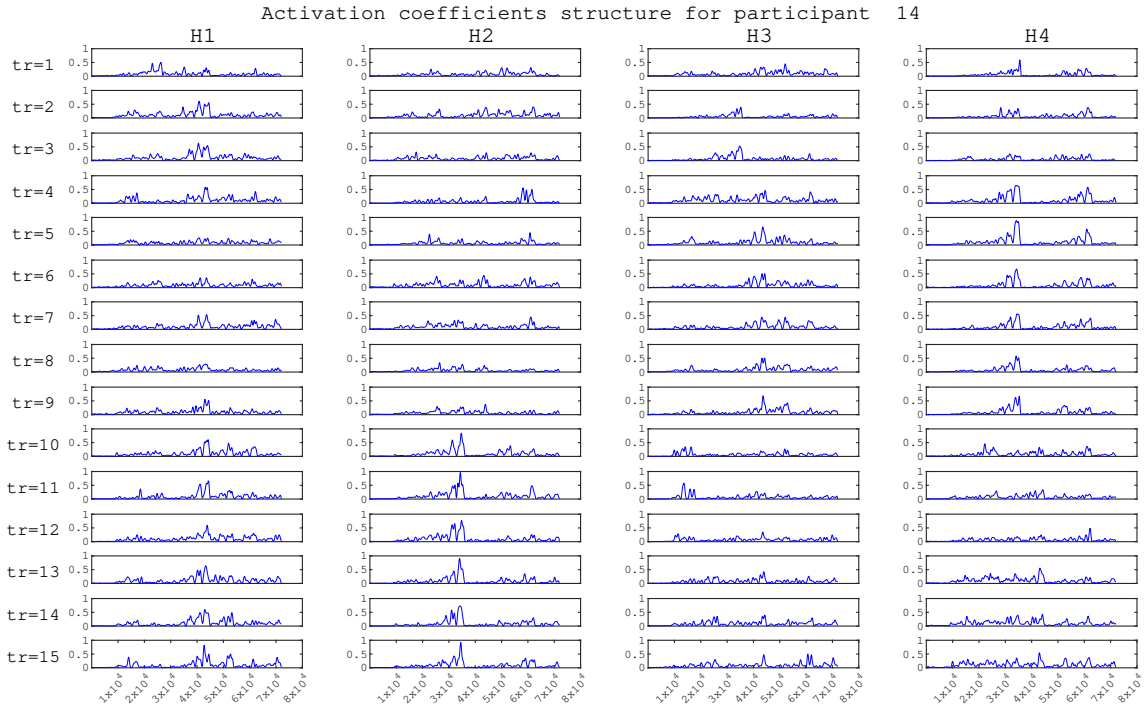


Figure 5.32: Change in four activation coefficient patterns (H1-H4) over training sessions (tr) for participant 14, matching is adopted from the matching of related muscle synergies, X-axis represents number of total observed points

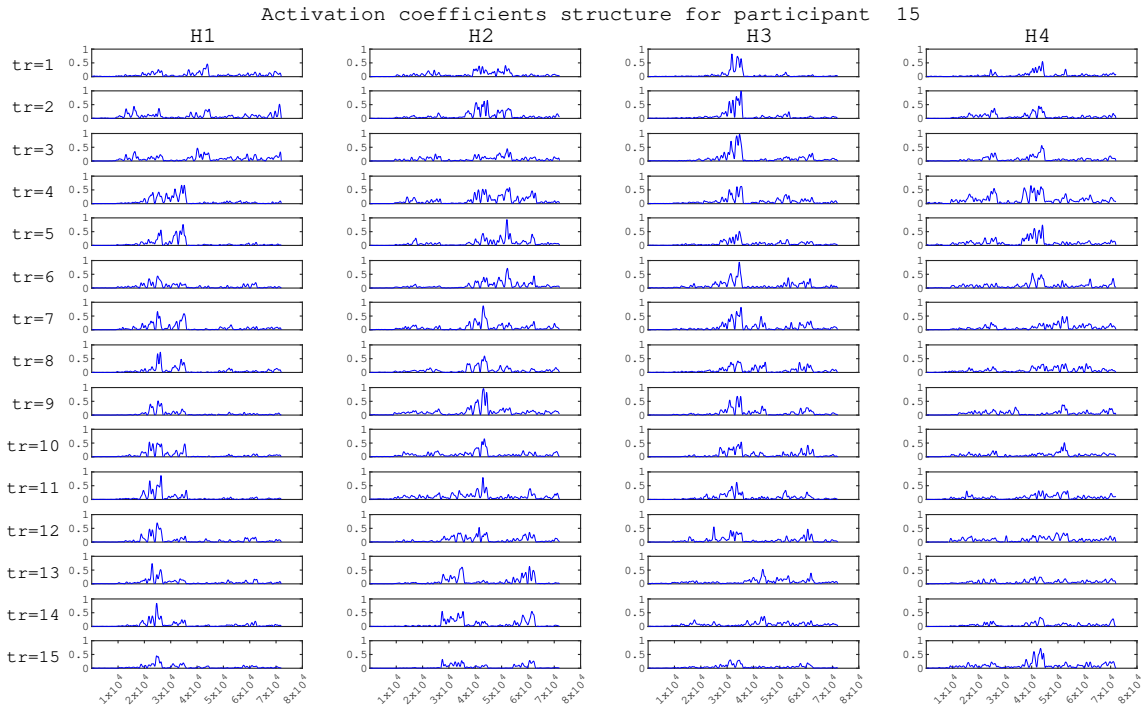


Figure 5.33: Change in four activation coefficient patterns (H1-H4) over training sessions (tr) for participant 15, matching is adopted from the matching of related muscle synergies, X-axis represents number of total observed points

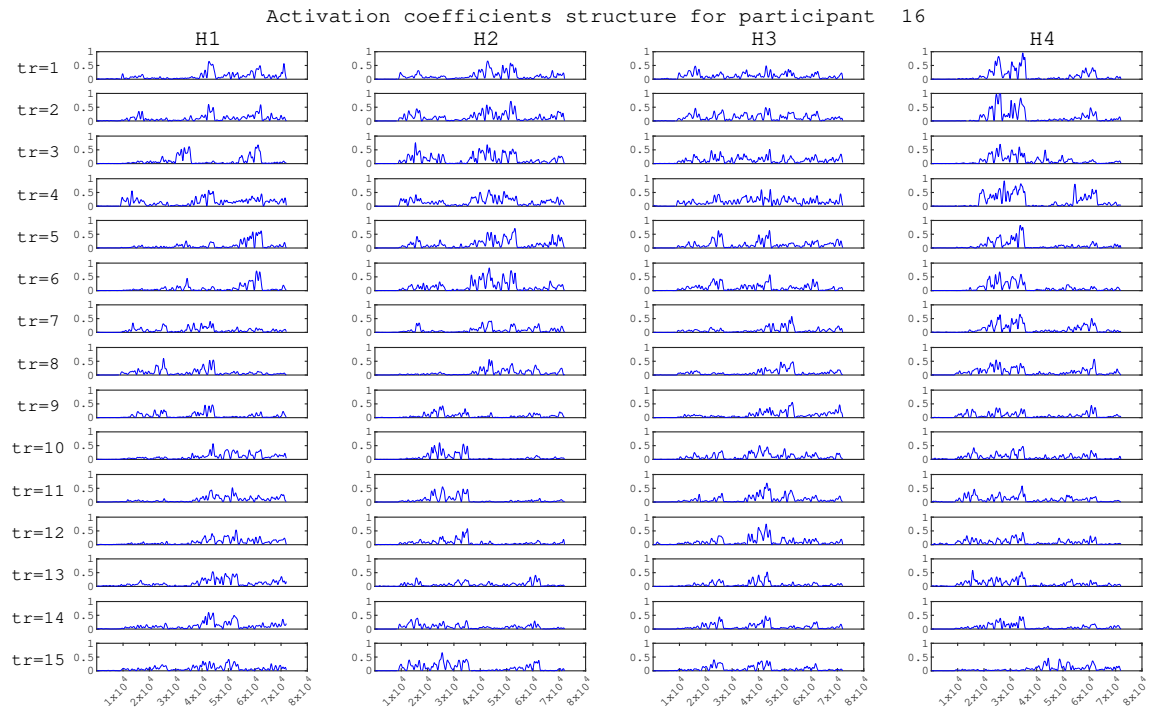


Figure 5.34: Change in four activation coefficient patterns (H1-H4) over training sessions (tr) for participant 16, matching is adopted from the matching of related muscle synergies, X-axis represents number of total observed points

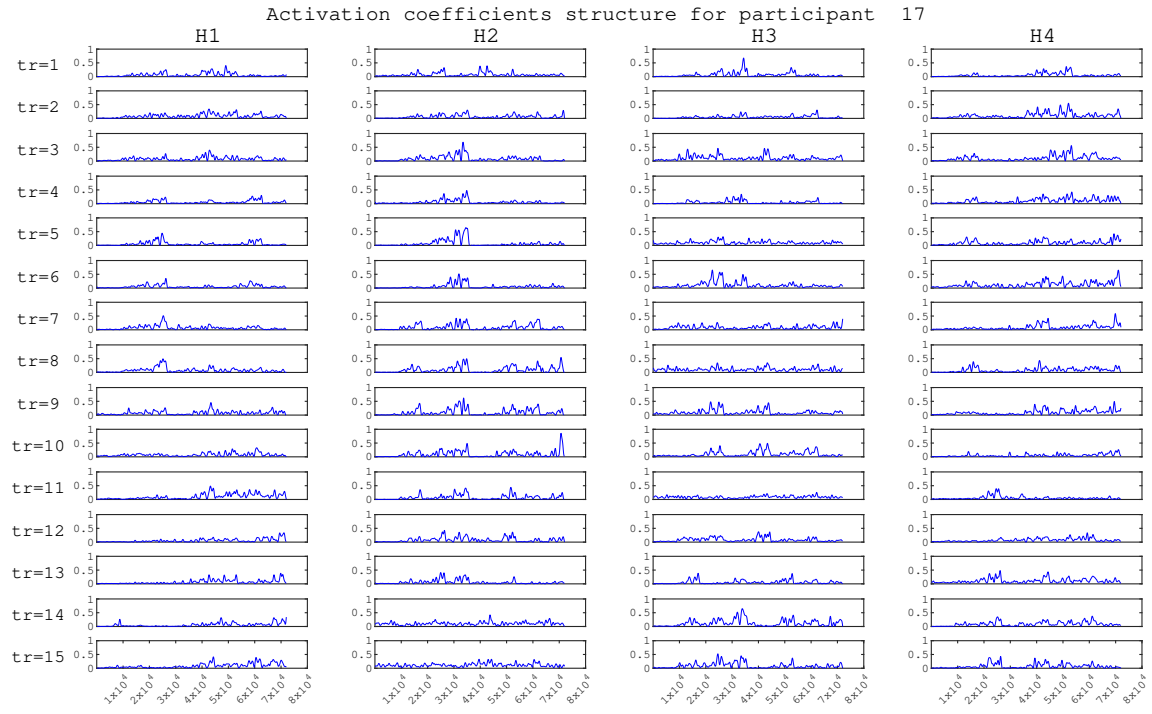


Figure 5.35: Change in four activation coefficient patterns (H1-H4) over training sessions (tr) for participant 17, matching is adopted from the matching of related muscle synergies, X-axis represents number of total observed points

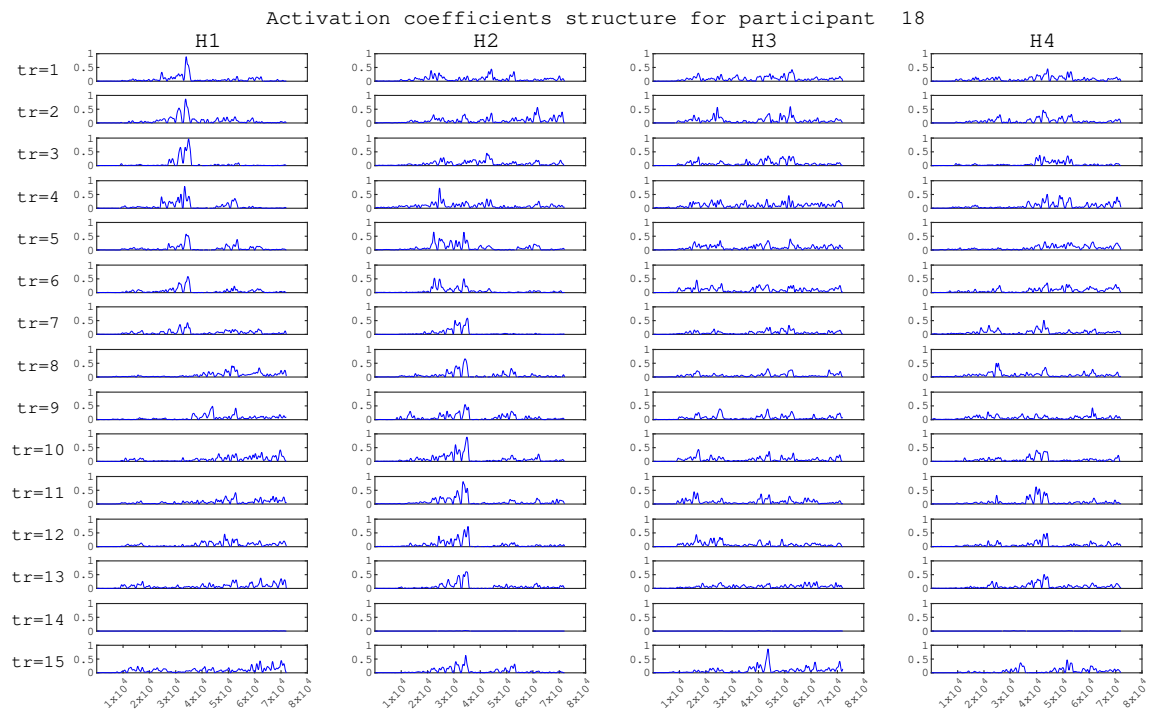


Figure 5.36: Change in four activation coefficient patterns (H1-H4) over training sessions (tr) for participant 18, matching is adopted from the matching of related muscle synergies, X-axis represents number of total observed points

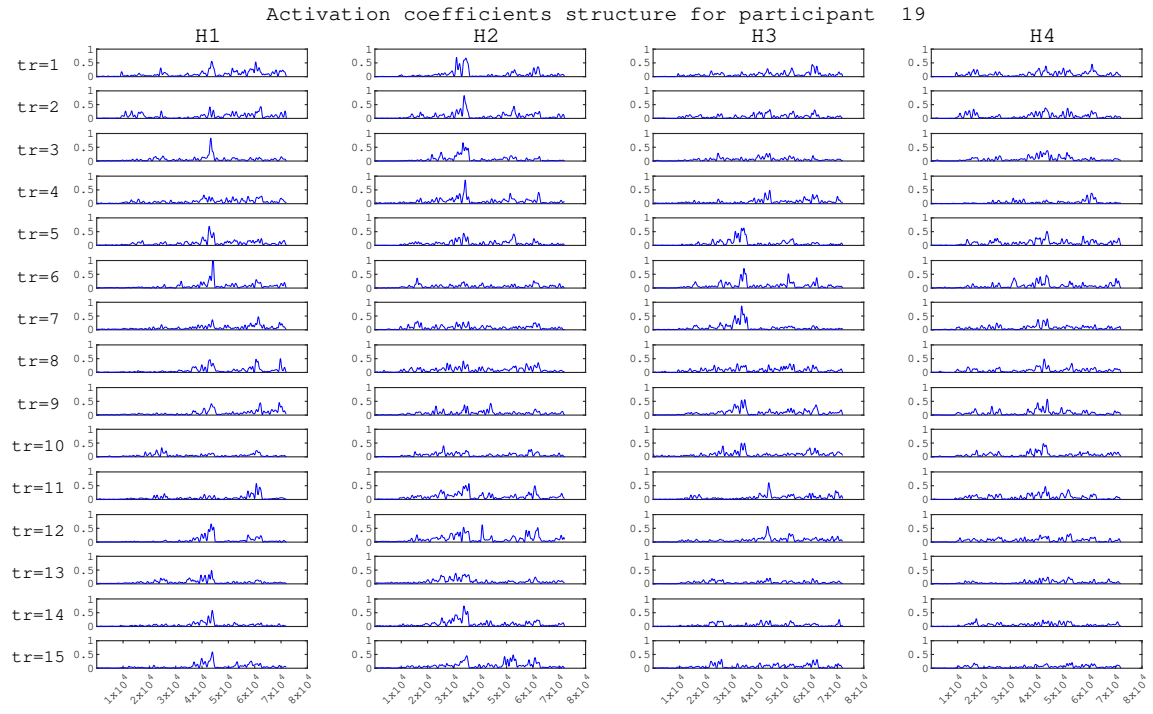


Figure 5.37: Change in four activation coefficient patterns (H1-H4) over training sessions (tr) for participant 19, matching is adopted from the matching of related muscle synergies, X-axis represents number of total observed points

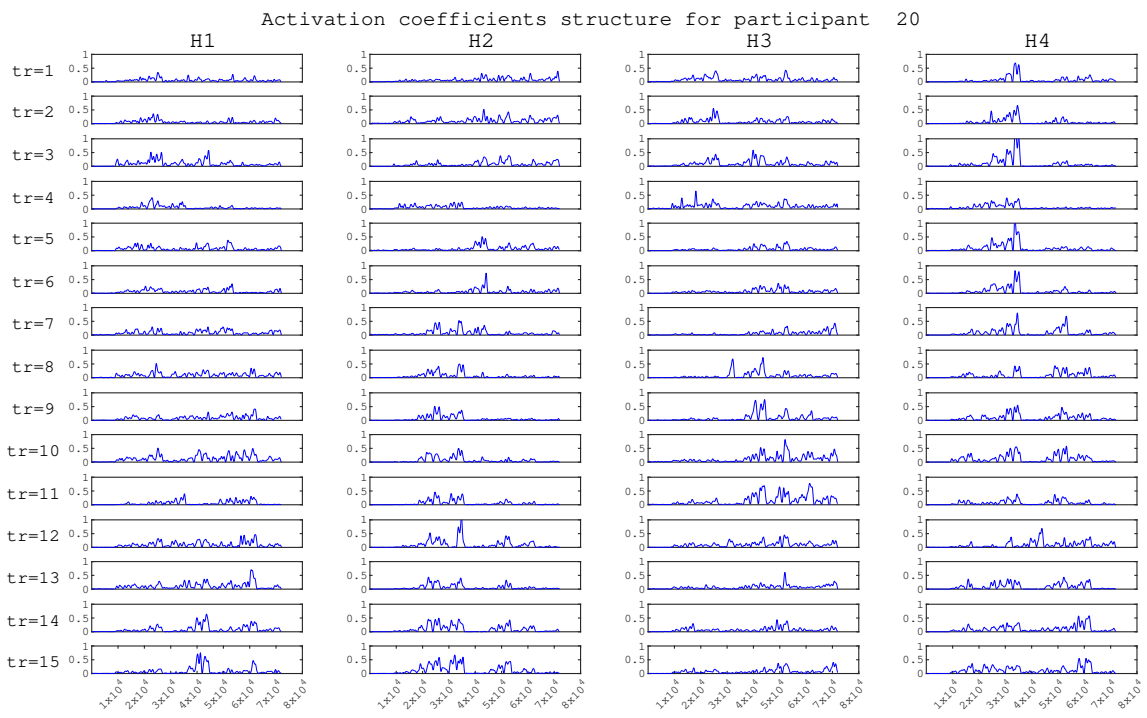


Figure 5.38: Change in four activation coefficient patterns (H1-H4) over training sessions (tr) for participant 20, matching is adopted from the matching of related muscle synergies, X-axis represents number of total observed points

Bibliography

- [1] M. B. Kristoffersen, A. W. Franzke, C. K. van der Sluis, A. Murgia, and R. M. Bongers, “The effect of feedback during training sessions on learning pattern-recognition-based prosthesis control”, *IEEE transactions on neural systems and rehabilitation engineering : a publication of the IEEE Engineering in Medicine and Biology Society*, vol. 27, no. 10, pp. 2087–2096, Oct. 2019, ISSN: 15580210. DOI: 10.1109/TNSRE.2019.2929917.
- [2] N. E. Bunderson and T. A. Kuiken, “Quantification of feature space changes with experience during electromyogram pattern recognition control.”, eng, *IEEE transactions on neural systems and rehabilitation engineering : a publication of the IEEE Engineering in Medicine and Biology Society*, vol. 20, no. 3, pp. 239–246, May 2012, ISSN: 1558-0210 (Electronic). DOI: 10.1109/TNSRE.2011.2182525.
- [3] M. A. Powell, R. R. Kaliki, and N. V. Thakor, “User training for pattern recognition-based myoelectric prostheses: Improving phantom limb movement consistency and distinguishability”, *IEEE Transactions on Neural Systems and Rehabilitation Engineering*, vol. 22, no. 3, pp. 522–532, 2014, ISSN: 15344320. DOI: 10.1109/TNSRE.2013.2279737.
- [4] E. Bizzi, A. D’Avella, P. Saltiel, and M. Tresch, “Book Review: Modular Organization of Spinal Motor Systems”, *The Neuroscientist*, vol. 8, no. 5, pp. 437–442, Oct. 2002, ISSN: 1073-8584. DOI: 10.1177/107385802236969. [Online]. Available: <http://journals.sagepub.com/doi/10.1177/107385802236969>.
- [5] M. C. Tresch, P. Saltiel, and E. Bizzi, “The construction of movement by the spinal cord”, *Nature Neuroscience*, vol. 2, no. 2, pp. 162–167, Feb. 1999, ISSN: 10976256. DOI: 10.1038/5721. [Online]. Available: https://www.nature.com/articles/nn0299%7B%5C_%7D162.
- [6] T. A. Valk, L. J. Mouton, E. Otten, and R. M. Bongers, “Fixed muscle synergies and their potential to improve the intuitive control of myoelectric assistive technology for upper extremities”, *Journal of NeuroEngineering and Rehabilitation*, vol. 16, no. 1, Jan. 2019, ISSN: 17430003. DOI: 10.1186/s12984-018-0469-5.

- [7] M. Ison and P. Artermiadis, *The role of muscle synergies in myoelectric control: Trends and challenges for simultaneous multifunction control*, Oct. 2014. DOI: 10.1088/1741-2560/11/5/051001.
- [8] F. Alnajjar, T. Wojtara, H. Kimura, and S. Shimoda, “Muscle synergy space: learning model to create an optimal muscle synergy”, *Frontiers in Computational Neuroscience*, vol. 7, no. OCT, p. 136, Oct. 2013, ISSN: 1662-5188. DOI: 10.3389/fncom.2013.00136. [Online]. Available: <http://journal.frontiersin.org/article/10.3389/fncom.2013.00136/abstract>.
- [9] M. Ison, I. Vujaklija, B. Whitsell, D. Farina, and P. Artermiadis, “High-Density Electromyography and Motor Skill Learning for Robust Long-Term Control of a 7-DoF Robot Arm”, *IEEE Transactions on Neural Systems and Rehabilitation Engineering*, vol. 24, no. 4, pp. 424–433, Apr. 2016, ISSN: 15344320. DOI: 10.1109/TNSRE.2015.2417775.
- [10] M. A. Powell and N. V. Thakor, “A Training Strategy for Learning Pattern Recognition Control for Myoelectric Prostheses”, Tech. Rep. 1, 2013, p. 30. [Online]. Available: http://www.oandp.org/jpo/library/printArticle.asp?printArticleId=2013%7B%5C_%7D01%7B%5C_%7D030.
- [11] S. M. Radhakrishnan, S. N. Baker, and A. Jackson, “Learning a Novel Myoelectric-Controlled Interface Task”, *Journal of Neurophysiology*, vol. 100, no. 4, pp. 2397–2408, Oct. 2008, ISSN: 0022-3077. DOI: 10.1152/jn.90614.2008. [Online]. Available: <https://www.physiology.org/doi/10.1152/jn.90614.2008>.
- [12] A. D’Avella, P. Saltiel, and E. Bizzi, “Combinations of muscle synergies in the construction of a natural motor behavior”, *Nature Neuroscience*, vol. 6, no. 3, pp. 300–308, Mar. 2003, ISSN: 10976256. DOI: 10.1038/nn1010.
- [13] F. R. Finley and R. W. Wirta, “Myocoder studies of multiple myopotential response.”, eng, *Archives of physical medicine and rehabilitation*, vol. 48, no. 11, pp. 598–601, Nov. 1967, ISSN: 0003-9993 (Print).
- [14] R. N. Scott, “MYOELECTRIC CONTROL OF PROSTHESES AND ORTHOSES”, Tech. Rep.
- [15] D. Farina, N. Jiang, H. Rehbaum, A. Holobar, B. Graimann, H. Dietl, and O. C. Aszmann, “The extraction of neural information from the surface EMG for the control of upper-limb prostheses: Emerging avenues and challenges”, *IEEE Transactions on Neural Systems and Rehabilitation Engineering*, vol. 22, no. 4, pp. 797–809, 2014, ISSN: 15344320. DOI: 10.1109/TNSRE.2014.2305111.
- [16] A. W. Franzke, M. Kristoffersen, V. Jayaram, C. van der Sluis, A. Murgia, and R. Bongers, “Exploring the relationship between EMG feature space characteristics and control performance in machine learning myoelectric control”, *IEEE Transactions on Neural Systems and Rehabilitation Engineering*, 2020.

- [17] A. D'Avella and F. Lacquaniti, *Control of reaching movements by muscle synergy combinations*, Apr. 2013. DOI: 10.3389/fncom.2013.00042.
- [18] Lena H. Ting and Stacie A. Chvatal, *Decomposing Muscle Activity in Motor Task: Motor Control: Theories, Experiments, and Applications*. Oxford Scholarship, 2010, pp. 103–138, ISBN: 9780195395273. [Online]. Available: <https://www.oxfordscholarship.com/view/10.1093/acprof:oso/9780195395273.001.0001/acprof-9780195395273-chapter-5>.
- [19] “Bioinformatics Toolbox™ User’s Guide R2018a”, Tech. Rep., 2003. [Online]. Available: www.mathworks.com.
- [20] S. Muceli, N. Jiang, and D. Farina, “Extracting signals robust to electrode number and shift for online simultaneous and proportional myoelectric control by factorization algorithms”, *IEEE Transactions on Neural Systems and Rehabilitation Engineering*, vol. 22, no. 3, pp. 623–633, 2014, ISSN: 15344320. DOI: 10.1109/TNSRE.2013.2282898.
- [21] D. D. Lee and H. S. Seung, *Algorithms for non-negative matrix factorization*, Jan. 2001. [Online]. Available: <https://collaborate.princeton.edu/en/publications/algorithms-for-non-negative-matrix-factorization>.
- [22] S. Muceli, A. T. Boye, A. D'Avella, and D. Farina, “Identifying representative synergy matrices for describing muscular activation patterns during multidirectional reaching in the horizontal plane”, *Journal of Neurophysiology*, vol. 103, no. 3, pp. 1532–1542, Mar. 2010, ISSN: 00223077. DOI: 10.1152/jn.00559.2009. [Online]. Available: www.jn.org.
- [23] M. C. Tresch, V. C. Cheung, and A. D'Avella, “Matrix factorization algorithms for the identification of muscle synergies: Evaluation on simulated and experimental data sets”, *Journal of Neurophysiology*, vol. 95, no. 4, pp. 2199–2212, Apr. 2006, ISSN: 00223077. DOI: 10.1152/jn.00222.2005. [Online]. Available: www.jn.org.
- [24] “Visual search: A large-scale perspective”, in *Handbook of Statistics*, vol. 31, Elsevier B.V., Jan. 2013, pp. 269–297. DOI: 10.1016/B978-0-444-53859-8.00011-4.
- [25] *Nonnegative matrix factorization - MATLAB nnmf - MathWorks Benelux*. [Online]. Available: <https://nl.mathworks.com/help/stats/nnmf.html> (visited on 07/08/2020).
- [26] M. W. Berry, M. Browne, A. N. Langville, V. Paul Pauca, and R. J. Plemmons, “Algorithms and Applications for Approximate Nonnegative Matrix Factorization”, Tech. Rep.
- [27] *Dot product - MATLAB dot - MathWorks Benelux*. [Online]. Available: <https://nl.mathworks.com/help/matlab/ref/dot.html> (visited on 07/08/2020).

-
- [28] Gene H. Golub and Charles F. Van Loan, *Matrix Computations — Johns Hopkins University Press Books*. [Online]. Available: <https://jhupbooks.press.jhu.edu/title/matrix-computations>.
 - [29] *k-Means Clustering - MATLAB & Simulink - MathWorks Benelux*. [Online]. Available: <https://nl.mathworks.com/help/stats/k-means-clustering.html> (visited on 07/08/2020).
 - [30] *Biopatrec/nmf_als.m at master · biopatrec/biopatrec*. [Online]. Available: https://github.com/biopatrec/biopatrec/blob/master/SigTreatment/Signal%20Separation/alg/nmf/nmf%7B%5C_%7Dals.m (visited on 07/08/2020).
 - [31] *Butterworth filter design - MATLAB butter - MathWorks Benelux*. [Online]. Available: <https://nl.mathworks.com/help/signal/ref/butter.html> (visited on 07/08/2020).
 - [32] *spider_plot - File Exchange - MATLAB Central*. [Online]. Available: https://nl.mathworks.com/matlabcentral/fileexchange/59561-spider%7B%5C_%7Dplot (visited on 07/08/2020).
 - [33] *Angle between two subspaces - MATLAB subspace - MathWorks Benelux*. [Online]. Available: <https://nl.mathworks.com/help/matlab/ref/subspace.html> (visited on 07/08/2020).
 - [34] *Motor Units and Muscle Receptors (Section 3, Chapter 1) Neuroscience Online: An Electronic Textbook for the Neurosciences — Department of Neurobiology and Anatomy - The University of Texas Medical School at Houston*. [Online]. Available: <https://nba.uth.tmc.edu/neuroscience/m/s3/chapter01.html> (visited on 07/08/2020).
 - [35] James A. Bourne and Marcello G.P. Rosa, “Hierarchical Development of the Primate Visual Cortex, as Revealed by Neurofilament Immunoreactivity: Early Maturation of the Middle Temporal Area (MT)”, *Cerebral Cortex*, vol. 16, no. 3, pp. 405–414, Mar. 2006. doi: 10.1093/CERCOR. [Online]. Available: <https://academic.oup.com/cercor/article/16/3/405/386350>.
 - [36] R. M. Bongers, P. J. Kyberd, H. Bouwsema, L. P. Kenney, D. H. Plettenburg, and C. K. Van Der Sluis, “Bernstein’s levels of construction of movements applied to upper limb prosthetics”, *Journal of Prosthetics and Orthotics*, vol. 24, no. 2, pp. 67–76, Apr. 2012, ISSN: 10408800. doi: 10.1097/JPO.0b013e3182532419.
 - [37] *Evaluate clustering solutions - MATLAB evalclusters - MathWorks Benelux*. [Online]. Available: <https://nl.mathworks.com/help/stats/evalclusters.html> (visited on 07/08/2020).
 - [38] K. R. Mills, *The basics of electromyography*, Jun. 2005. doi: 10.1136/jnnp.2005.069211. [Online]. Available: www.jnnp.com.

- [39] E. Stålberg, H. van Dijk, B. Falck, J. Kimura, C. Neuwirth, M. Pitt, S. Podnar, D. I. Rubin, S. Rutkove, D. B. Sanders, M. Sonoo, H. Tankisi, and M. Zwarts, *Standards for quantification of EMG and neurography*, Sep. 2019. DOI: 10.1016/j.clinph.2019.05.008.